JOURNAL OF GEOPHYSICAL RESEARCH, VOL. 97, NO. D18, PAGES 20,647–20,670, DECEMBER 20, 1992

Tropospheric Chemistry Over the Lower Great Plains of the United States 2. Trace Gas Profiles and Distributions

WINSTON T. LUKE[1], RUSSELL R. DICKERSON, WILLIAM F. RYAN, KENNETH E. PICKERING[2], AND LINDA J. NUNNERMACKER[3]

University of Maryland, College Park, Maryland

Convective clouds and thunderstorms redistribute air pollutants vertically, and by altering the chemistry and radiative balance of the upper troposphere, these local actions can have global consequences. To study these effects, measurements of trace gases ozone, O_3, carbon monoxide, CO, and odd nitrogen were made aboard the NCAR Sabreliner on 18 flights over the southern Great Plains during June 1985. To demonstrate chemical changes induced by vertical motions in the atmosphere and to facilitate comparison with computer model calculations, these data were categorized according to synoptic flow patterns. Part 1 of this two-part paper details the alternating pulses of polar and maritime air masses that dominate the vertical mixing in this region. In this paper, trace gas measurements are presented as altitude profiles (0-12 km) with statistical distributions of mixing ratios for each species in each flow pattern. The polar flow regime is characterized by northwesterly winds, subsiding air, and convective stability. Concentrations of CO and total odd nitrogen (NO_y) are relatively high in the shallow planetary boundary layer (PBL) but decrease rapidly with altitude. Ozone, on the other hand, is uniformly distributed, suggesting limited photochemical production; in fact, nitric oxide, NO, mixing ratios fell below 10 ppt (parts per 10^{12} by volume) in the midtroposphere. The maritime regime is characterized by southerly surface winds, convective instability, and a deep PBL; uniformly high concentrations of trace gases were found up to 4 km on one flight. Severe storms occur in maritime flow, especially when capped by a dry layer, and they transport large amounts of CO, O_3, and NO_y into the upper troposphere. Median NO levels at high altitude exceeded 300 ppt. Lightning produces spikes of NO (but not CO) with mixing ratios sometimes exceeding 1000 ppt. This flow pattern tends to leave the midtroposphere relatively clean with concentrations of trace gases similar to those observed in the polar category. During frontal passage both stratiform and convective clouds mix pollutants more uniformly into the middle and upper levels; high mixing ratios of CO are found at all altitudes, and O_3 levels are highest of any category, implicating photochemical production. These results illustrate the importance of convection in tropospheric chemistry. Use of average trace gas profiles or eddy diffusion parameterized vertical mixing can lead to errors of 30 to 50% in O_3 and CO concentrations and an order of magnitude for odd nitrogen.

1. INTRODUCTION

This is the second of a two-part paper describing the meteorology and tropospheric chemistry of the south central United States during summer, focusing on the role of convection in the distribution of photochemically active pollutants. Because long-term monitoring of trace gas profiles is impractical, part 1 [*Ryan et al.*, 1992] develops a regional climatology with emphasis on vertical mixing. Here, we present altitude profiles and statistics of trace gas mixing ratios characteristic of those climatological categories in order to understand better the physical processes that control the chemical composition of the atmosphere.

Part 1 describes the meteorology during the 18 research flights and provides a summary of the objectives and key components of the Preliminary Regional Experiment for STORM-CENTRAL (PRE-STORM) and Processing of Emissions by Clouds and Precipitation (PRECP) experiments. Table 1 lists the date and synoptic flow category for each flight; lightning data are discussed below. Detailed analyses of individual flights may be found in the work of *Dickerson et al.* [1987], *Pickering* [1987], *Pickering et al.* [1988, 1989, 1990], and *McNamara* [1988].

2. EXPERIMENTAL METHODS

Trace gas measurements described in this paper were made aboard a North American Rockwell Sabreliner, a twin-jet aircraft operated by the National Center for Atmospheric Research (NCAR). The starting time, duration, maximum altitude, and latitude/longitude range of each Sabreliner flight may be found in part 1. Research flights were typically 2-2.5 hours in duration and were generally conducted over Oklahoma and Kansas.

2.1. *Trace Gas Instrumentation*

Reactive nitrogen compounds, ozone (O_3), and carbon monoxide (CO) were monitored with continuous techniques; nonmethane hydrocarbons (NMHCs; results published previously by *Pickering et al.* [1990]) were collected at discrete points along the flight path. More detailed information about the deployment and calibration of all the instruments as well as data reduction techniques may be found in the works by *Luke* [1990] and *Pickering* [1987].

Ozone. Ozone was measured by an ultraviolet absorption photometer (Model 1003-AAS airborne ozone detector, Dasibi Environmental Corporation, Glendale, California) modified for

[1]Now at NOAA, Air Resources Laboratory, Silver Spring, Maryland.

[2]Now at Universities Space Research Association, NASA Goddard Space Flight Center, Greenbelt, Maryland.

[3]Now at Brookhaven National Laboratory, Upton, New York.

Paper number 92JD02127.
0148-0227/92/92JD-02127$05.00

TABLE 1. Research Flights Made by the Sabreliner During PRESTORM 1985

Flight	Date	Classification	Lightning
F1	June 3	mT	3554
R1	June 5	fropa	ND
R2	June 8	scrubbed	• • •
R3	June 10	mT(mod)	848
R4	June 10	mT(mod)	23
R5	June 13	P(mod)	0
R6	June 15	MCS	2000
R7	June 16	mT(mod)	ND
R8	June 17	mT(mod)/fropa	ND
R9	June 17	fropa	ND
R10	June 18	fropa/P	101
R11	June 20	P(mod)	0
R12	June 22	mT	1306
R13	June 22	mT	2
R14	June 25	mT(mod)	ND
R15	June 26	mT/fropa	2978
R16	June 26	mT/fropa	5954
R17	June 27	fropa/P	38
F2	June 28	P	0

Lightning refers to the number of cloud-to-ground flashes near the flight region for the time of the flight and the previous 6 hours as recorded by the NSSL network. "ND" means no data on lightning were recorded that day. Data for flight R6 are estimated from hard copy obtained on the day of the flight but not recorded on tape.

fast response. The detector is capable of measuring as little as 3 ppb (parts per 10^9 by volume) of O_3 in 7 s, and the uncertainty of the data presented here is $\pm 10\%$. The raw detector output was corrected for cabin temperature and pressure. Ambient airflow to the O_3 and CO detectors was delivered by the engines' compressors through the cabin ventilation system. While carbon monoxide is a robust gas which remains undisturbed during its travel through the jet intakes, ozone concentrations were corrected for a small degree of ozone destruction on the compressor blades during level flight and for slightly increased destruction during aircraft ascents. Additional details may be found in *Pickering* [1987] and *Luke* [1990].

Carbon monoxide. A commercial gas filter correlation, nondispersive infrared detector, modified for enhanced sensitivity [*Dickerson and Delany*, 1988] was used to measure tropospheric CO. The detector (model 48, Thermo Environmental, Franklin, Massachusetts) measures CO from the absorption of 4.67 μm radiation by a fundamental vibration- rotation band of CO. The residual interference from H_2O vapor is removed by continuously drying the sample air with molecular sieve 4A, and the detector zero is established with Hopcalite (Mine Safety Appliances, Pittsburgh, Pennsylvania). An internal microcomputer automatically corrects the detector output for temperature and pressure using built-in transducers. Data were recorded every second and averaged over 30 s, the time required to register 50% of a step change. For 30-s averages the noise ($\pm 2\sigma$) under the flight conditions is approximately 30 ppb CO. Calibrations performed in the laboratory both before and after the field experiment using a National Institute of Standards and Technology (NIST) standard reference material (CO/N_2 balance, SRM 23-49-D; see *Hughes et al.* [1991]) varied by less than 2.5%.

Reactive nitrogen. Reactive nitrogen compounds were measured with a commercial ozone chemiluminescence detector [e.g., *Fontijn et al.*, 1970; *Stedman et al.*, 1972] modified for enhanced sensitivity [*Delany et al.*, 1982; *Dickerson et al.*, 1984]. This instrument (model 14B, Thermo Environmental, Franklin, Massachusetts) has been described by *Luke and Dickerson* [1987], *Pickering et al.* [1988], and *Luke* [1990] and will be briefly reviewed below.

A schematic diagram (Figure 1) shows the two rear-facing inlets used to draw ambient air into the detector without sampling coarse aerosols and cloudwater droplets. The inlets were mounted on an aperture atop the Sabreliner fuselage, approximately 270 cm from the aircraft's nose and well ahead of the jet intakes. The central axis of each inlet rests approximately 25 cm above the fuselage, well out of the aircraft's boundary layer.

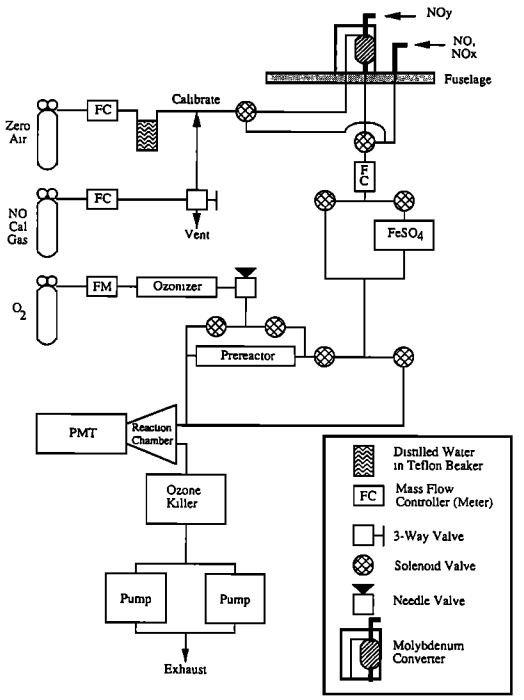

Fig. 1. Schematic diagram of chemiluminescence detector used to measure oxides of nitrogen during PRESTORM. All materials were composed of quartz, Teflon, or stainless steel. Inlets faced the rear of the aircraft.

The first inlet system is composed of a 6.4-mm OD stainless steel tube. The incoming air sample is routed through a series of Teflon solenoid valves (Nacom Industries, Tustin, California), either to a stainless steel prereactor where nitric oxide (NO) reacts with O_3 out of sight of the photomultiplier tube to generate a chemical zero (background mode), directly to the reaction chamber (NO mode), or to a quartz vessel containing approximately 28 g of crystalline ferrous sulfate, $FeSO_4 7\ H_2O$ (NO_x* mode). A second inlet allows for the measurement of total reactive nitrogen (NO_y mode; see below). The instrument stays in each mode for 3 min, and a complete measurement cycle lasts 12 min.

Ferrous sulfate efficiently reduces NO_2 to NO [*Kelly et al.*, 1980; *Fehsenfeld et al.*, 1987; *Nunnermacker*, 1990] but suffers from a peroxyacetyl nitrate (PAN) interference [*Fehsenfeld et al.*, 1987]. Recent tests in our laboratory indicate that under typical experimental conditions described in this paper, PAN is converted to NO with 75 to 95% efficiency. The $RONO_2$ interference on $FeSO_4$ reported in *Fehsenfeld et al.* [1987] was not demonstrated in recent laboratory tests [*Nunnermacker*,

1990]. In the background troposphere, PAN concentrations may approach or exceed those of NO_x (NO_x = NO + NO_2) [*Singh and Hanst*, 1981; *Singh and Salas*, 1983; *Singh et al.*, 1985; *Ridley et al.*, 1990]. We believe that the signal arising from conversion on $FeSO_4$ is most accurately represented by the sum of NO, NO_2, and PAN (NO_x* = NO + NO_2 + PAN). (The reader is referred to *Nunnermacker* [1990], *Fehsenfeld et al.* [1987], and references therein for further details.) NO_x* data are included here for comparison with earlier measurements made with $FeSO_4$ [*Dickerson*, 1984, 1985; *Kondo et al.*, 1987; *Misanchuk et al.*, 1987; *Luke and Dickerson*, 1987; *Hastie et al.*, 1988]. The efficiency of NO_2 conversion on the $FeSO_4$ catalyst was determined by gas phase titration [*Stedman*, 1976] to be 99% before and 98% after the field project.

An externally mounted molybdenum (Mo) converter [*Dickerson et al.*, 1987; *Fehsenfeld et al.*, 1987; *Luke and Dickerson*, 1987; *Luke*, 1990; *Nunnermacker*, 1990] forms the second inlet system and is used to measure total reactive nitrogen (NO_y mode; NO_y = NO + NO_2 + NO_3 + HONO + HNO_3 + HO_2NO_2 + 2 N_2O_5 + PAN + R-ONO_x + fine p-NO_3^-). Approximately 15 g of Mo is housed in a quartz reaction vessel with a 1-cm OD inlet and is heated to 375°C. The inlet is short (5 cm length) to avoid losses of reactive species such as HNO_3. Ambient levels of NO_y measured with this converter agreed well with those measured by a Au/CO oxidation technique [*Fehsenfeld et al.*, 1987] at NO_y concentrations ranging from 0.2 to 100 ppb. Conversion of reactive nitrogen species to NO is virtually quantitative, while the oxidation of reduced nitrogen species is negligible at the optimum operating temperature of 375°C [*Nunnermacker*, 1990; *Fehsenfeld et al.*, 1987; and references therein]. The NO_2 conversion efficiency of the molybdenum catalyst was measured to be 95% and 97% (with 5% uncertainty) before and after the project, respectively.

The NO detector was operated with a 2-s time response; its analog output signal was sampled at 1 Hz and filtered at 10-s intervals. Under aircraft conditions the detection limit at the 95% confidence level, defined as a signal-to-noise ratio of unity for $\pm 2\sigma$ of the noise level in the background mode, is approximately 20 ppt (parts per 10^{12} by volume) NO for a 10-s integration time. The detection limit can be reduced with longer averaging times, for example, the detection limit is about 5 ppt when fifteen 10-s averages are combined. Noise from sources other than the background signal, such as cosmic rays and NMHCs, begin to become important at longer averaging times. In this paper, reactive nitrogen mixing ratios are presented with 1 ppt resolution for numerical accuracy, but resolution below about 5 ppt is not statistically significant. We estimate the uncertainty of the measurements to be approximately ±15% for NO and ±25% for NO_y (see *Fehsenfeld et al.* [1987] and *Nunnermacker* [1990] for further details).

The NO detector was calibrated in flight at the 0.6-6.0 ppb level by dynamically diluting a secondary NO standard (Scott Specialty Gases, Plumbsteadville, Pennsylvania) with a larger flow of zero air. Reference against a NIST standard reference material (NO/N_2 balance, SRM 48-55BL) showed that the calibration gas contained 1.47 ppm (parts per 10^6 by volume) NO. On the only research mission flown at night (R16), NO was below the detection limit after sunset, indicating no measurable instrument artifact.

Due to the extreme variability of water vapor concentration in the troposphere, a small flow of humidified air (100 cm^3 min^{-1} at STP) was added at the detector inlet to keep the humidity of the sample air stream within a narrow range. A moistened airflow ensures rapid conversion of NO_2 on $FeSO_4$, minimizes the memory effect of the molybdenum converter, helps keep the sensitivity of NO detection constant, reduces background noise, and minimizes the conversion of reduced nitrogen species on the heated molybdenum catalyst [*Carroll et al.*, 1985; *Dickerson*, 1985; *Drummond et al.*, 1985; *Fehsenfeld et al.*, 1987; *Nunnermacker*, 1990]. Finally, the instrument was flushed with zero air during takeoff and landing to prevent contamination in the polluted airport environment.

3. Results and Discussion

In order to organize the substantial data set collected during 18 flights of the Sabreliner (Table 2) the trace gas mixing ratios were first placed within the appropriate meteorological context [*Ryan et al.*, this issue]. The flights were separated according to the meridional flow into polar (P) or maritime tropical (mT) categories. Within these general flow patterns, subcategories representing modified conditions (P(mod), mT(mod)) were identified. Episodes of frontal passage (fropa) mark the transition between the categories. Each trace gas observation was then placed into one of 10 layers (abbreviated L1 to L10) of equal pressure thickness (~82 mbar), based on the pressure altitude of the observation (*NOAA, U.S. Standard Atmosphere*, 1976); see Table 3. The great majority of NO observations were made when the solar zenith angle was less than 40°; thus no correction is made for the variable rate of NO_2 photolysis.

TABLE 2. Number of Trace Gas Observations in each Branch and Subphase of the Meridional Circulation Over the Flight Region

	Number of Observations				
Category	NO	NO_x*	NO_y	CO	O_3
mT	188	411	178	419	2671
mT(mod)	405	510	622	465	5119
Fropa	550	775	911	811	5592
P	11	177	0	112	694
P(mod)	130	500	348	291	2450
All Flights	1284	2373	2059	2098	16526

The duration of each observation was 7 s for ozone, 10 s for odd nitrogen, and 30 s for carbon monoxide.

TABLE 3. Pressure and Altitude Ranges for Equal-Mass Layers

Layer	Pressure,mbar	Altitude,m
1	1013-931	0-708
2	931-849	708-1467
3	849-767	1467-2287
4	767-685	2287-3182
5	685-603	3182-4168
6	603-521	4168-5270
7	521-439	5270-6522
8	439-357	6522-7981
9	357-275	7981-9741
10	275-193	9741-12010

The synoptic conditions accompanying the convective storm studied by *Dickerson et al.* [1987] as part of this project do not fit into any of the five categories used here (see part 1); however, the chemistry and mesoscale dynamics of that storm most closely resemble mT(mod) conditions.

3.1. *Trace Gas Profiles*

For 17 research flights the mean and standard deviation of the observed NO, NO_x*, and NO_y concentrations are listed as a function of flow regime and layer number in Table 4, while median and quartiles are listed in Table 5. Note that NO, NO_x*, and NO_y were not measured simultaneously, and were sometimes highly variable (especially around lightning); thus it is possible for [NO] within a given layer to be greater than [NO_x*]. Mean CO and O_3 concentrations are listed in Table 6,

TABLE 4. Mean Mixing Ratios and Standard Deviations (in ppt) of NO, of NO, NO_x*, and NO_y in Each Equal-Mass Layer and Synoptic Phase of the Meridional Circulation Over the Flight Region

Layer	P/P(mod)	mT	mT(mod)	Fropa
		NO, ppt		
1	• • •	• • •	• • •	• • •
2	85±14(13)	• • •	85±10(14)	360±255(28)
3	• • •	• • •	• • •	78*
4	23±7(16)	• • •	46±8(15)	51±34(35)
5	• • •	• • •	13(2)	42±21(22)
6	• • •	• • •	21±3(6)	• • •
7	19±12(15)	50±10(12)	22±9(22)	44±56(76)
8	4±5(15)	106±103(57)	231±799(121)	147±203(62)
9	49±16(27)	165±111(58)	86±119(97)	56±56(141)
10	60±45(55)	496±409(61)	153±163(128)	183±123(184)
		NO_x, ppt*		
1	• • •	• • •	• • •	• • •
2	1370±1060(99)	1155±408(46)	620±38(15)	1770±786(25)
3	606±291(77)	857±392(49)	• • •	676±179(14)
4	343±196(155)	690±463(53)	226±63(30)	448±373(37)
5	315±121(93)	803±418(40)	• • •	317±131(44)
6	353±163(48)	451±340(50)	310±55(31)	276±42(34)
7	160±46(52)	272±134(36)	292±28(31)	212±90(143)
8	172±77(82)	647±172(16)	444±614(116)	435±189(90)
9	233±85(44)	752±605(68)	366±146(138)	328±337(232)
10	360±141(27)	446±375(53)	461±231(149)	472±261(156)
		NO_y, ppt		
1	• • •	• • •	• • •	• • •
2	1830±576(75)	• • •	1460±239(30)	4080±1210(48)
3	1740±301(44)	• • •	1320±207(4)	1640±471(10)
4	791±294(56)	• • •	928±264(23)	1120±223(37)
5	889±216(46)	• • •	883±9(3)	1470±590(36)
6	640±184(52)	• • •	1390±304(37)	580±308(19)
7	315±127(18)	864±528(33)	1070±354(19)	842±354(93)
8	318±55(24)	1520±570(25)	922±684(103)	1048±349(136)
9	240±25(15)	1790±639(60)	1160±592(177)	918±593(377)
10	803±111(18)	903±480(60)	1010±680(226)	1130±398(155)

Mean and standard deviation of observed trace gas concentrations in 1985. The number of 10-s measurements in each layer is listed within parentheses. Standard deviations are omitted for samples of fewer than 3 data points.

and median concentrations may be found in Table 7. In general, the trace gas data are not described by normal distributions. The following discussion will thus focus on median, rather than mean, concentrations.

While several thousand individual trace gas measurements were recorded (see Table 2), it must be remembered that these observations are not independent. The number of independent observations, also referred to as the number of degrees of freedom in the measurements, is much less than the number of trace gas observations. Estimating the degrees of freedom in the present data set is difficult, but we will assume that the number of independent observations in each flow regime is equal to the number of research flights or flight segments in that category. Given this restriction and the large horizontal spatial variability in trace gas concentrations induced by cloud vertical transport, our observations illustrate the effects of vertical and horizontal atmospheric motions upon trace gas concentrations and tropospheric photochemistry.

Polar flow (P and P(mod)). As noted in part 1, the steep increase of equivalent potential temperature (θ_e) with altitude in P and P(mod) flow produces convective stability above the lowest layers. Wind direction data from the Oklahoma City rawinsondes and the alignment of the isobars on the National Weather Service (NWS) upper level charts suggest trajectories from the sparsely populated regions to the west and northwest of the flight region. The convective stability of polar flow largely confines surface emissions of pollutants to the shallow mixed layer, where they are more efficiently removed by heterogeneous processes and gas phase photooxidation mechanisms. Vertical transport under these conditions of gentle subsidence is very slow; concentrations of reactive trace gases emitted at the surface should decrease sharply with altitude [e.g., *Chameides and Cicerone*, 1978] and display uniformly low mixing ratios in the free troposphere.

The profile of carbon monoxide in polar flow agrees with expectations and is characterized by a substantial vertical concentration gradient (Figure 2*a*). (To achieve better coverage, data from the P and P(mod) subcategories were combined and are denoted as P/P(mod) in this figure.) Mixing ratios of CO decrease rapidly with altitude; the median [CO] in *P* flow drops from 142 ppb in L2 to 120 ppb in L4 and then to 69 ppb in L9 (Table 7).

The increasing [CO] gradient in L9 and L10 (see Tables 6 and 7) would appear inconsistent with the negative gradient observed throughout much of the troposphere under polar flow conditions. Careful examination of the synoptic conditions shows that the air in these layers had an unusual history. Data in L9 and L10 derive exclusively from flights R17 and R5. On R17 (P flow), CO was measured in a thin cirrus deck in the polar air behind the leading edge of a surface cold front, and the high [CO] is attributed to the vertical displacement of lower tropospheric air along the frontal zone. On R5 (P(mod) flow), isentropic back trajectory analysis [*Pickering et al.*, 1989] revealed that the air in L9 and L10 had been injected into the upper troposphere by earlier convective activity near Denver, 600 km upstream of the flight region. The local maxima in mean [NO_x*] and [CO] in L6 (see Tables 5 and 6) also result from this upstream convective activity; removing these data reduces the average NO_x* and CO concentrations in L6 to 225 ±107 ppt and 90 ±14 ppb, respectively.

In the absence of pollution and vertical transport, profiles of reactive nitrogen concentrations should resemble a "C" shape, reflecting inputs in the upper and lower troposphere (strato-

TABLE 5. Median Mixing Ratios (ppt) of NO, NO_x^*, and NO_y in Each Equal-Mass Layer and Synoptic Phase of the Meridional Circulation

	Median Trace Gas Concentrations			
Layer	P/P(mod)	mT	mT(mod)	Fropa
		NO, ppt		
1	• • •	• • •	• • •	• • •
2	87(67-98)	• • •	90(69-96)	219(100-640)
3	• • •	• • •	• • •	78(73-83)
4	22(14-32)	• • •	45(34-54)	48(16-76)
5	• • •	• • •	14(0-14)	46(14-68)
6	• • •	• • •	21(17-22)	• • •
7	22(3-31)	50(39-61)	22(12-33)	20(6-78)
8	3(-3-8)	93(6-182)	28(5-93)	109(41-212)
9	48(32-68)	127(85-242)	66(19-109)	43(0-113)
10	60(11-97)	312(87-1030)	97(33-233)	168(55-291)
		NO_x^* ppt		
1	• • •	• • •	• • •	• • •
2	676(572-2009)	1250(649-1615)	627(566-653)	1736(950-2188)
3	536(345-872)	744(401-1435)	• • •	639(517-746)
4	322(155-564)	529(285-1422)	213(173-256)	263(129-927)
5	297(204-458)	589(404-1349)	• • •	288(183-481)
6	406(159-509)	251(182-815)	303(283-336)	275(234-306)
7	164(112-207)	246(131-396)	286(264-328)	192(120-299)
8	161(103-243)	691(519-739)	293(217-412)	389(287-549)
9	240(123-326)	558(431-1108)	355(258-470)	296(102-407)
10	294(251-558)	231(134-849)	372(252-681)	405(233-671)
		NO_y, ppt		
1	• • •	• • •	• • •	• • •
2	1529(1314-2495)	• • •	1383(1272-1587)	3972(3284-4764)
3	1802(1396-1926)	• • •	1337(1060-1555)	1717(905-2154)
4	869(387-1026)	• • •	814(681-1246)	1073(886-1323)
5	942(604-1068)	• • •	884(874-892)	1334(890-2040)
6	662(528-755)	• • •	1402(971-1712)	706(209-886)
7	279(256-288)	606(521-1608)	1088(564-1349)	724(581-1242)
8	340(247-368)	1670(682-2034)	687(303-1461)	1038(695-1454)
9	238(208-272)	1660(1310-2309)	1229(461-1757)	743(615-1098)
10	843(625-874)	643(503-1445)	810(572-1324)	998(766-1548)

The range spanned by the first and third quartiles (25% and 75% percentiles) is in parentheses.

sphere and soils, respectively) and the dearth of sources in the middle troposphere [e.g., *Kley et al.*, 1981; *Drummond et al.*, 1988]. Vertical profiles of reactive nitrogen compounds in P/P(mod) flow (Figures 2*b* and 3) define minima in the middle troposphere (L7 and L8), generally coincident with the CO minimum and consistent with expectations.

The small coefficients of variability (ratio of the standard deviation to the mean) reflected in P/P(mod) odd nitrogen data also illustrate the unperturbed nature of the convectively stable polar air (Table 4). The variability of trace gas concentrations varies inversely with residence time [e.g., *Junge*, 1974], and NO_x* data collected under numerous P/P(mod) episodes exhibit standard deviations among the lowest recorded for all meridional airflow categories. The small variation in the data suggests that the polar air was unaffected by convective mixing within the lifetime of NO_x*, consistent with expectations.

The typically small coefficients of variability of P(mod) ozone concentrations (Table 6) suggest few recent stratospheric inputs of O_3 and, combined with the low odd nitrogen and CO mixing ratios, imply that only limited photochemical O_3 production occurs in this clean air advected from higher latitudes. While the precise concentration is below our detection limit, the extremely low average NO mixing ratio in L8 (the average of 15 observations is 4 ppt) suggests that some photochemical destruction may even occur. The dramatic increase in $[O_3]$ in L10, especially in P(mod) flow (Figure 4), reflects the reduced height of the tropopause in the postfrontal environment [part 1] and air of stratospheric origin.

TABLE 6. Mean Mixing Ratios and Standard Deviations (ppb) of CO and O_3 in Each Equal-Mass Layer and Synoptic Phase of the Meridional Circulation Over the Flight Region

Layer	P	P(mod)	mT	mT(mod)	Fropa
			CO, ppb		
1	163±14(3)	• • •	• • •	• • •	• • •
2	147±34(6)	157±40(59)	140±14(19)	124±31(32)	190±40(51)
3	148±24(4)	134±24(24)	118±19(23)	124±21(16)	128±39(26)
4	131±25(7)	119±24(60)	128±21(17)	98±18(21)	121±11(56)
5	125±24(16)	94±19(25)	140±19(14)	96±11(5)	128±12(31)
6	119±25(16)	102±28(32)	100±23(24)	93±17(15)	122±12(16)
7	106±17(15)	87±13(46)	101±21(61)	107±14(28)	107±16(114)
8	87±17(21)	89±15(22)	95±12(75)	101±18(93)	114±15(88)
9	72±15(15)	97±5(6)	99±17(87)	106±22(132)	105±22(221)
10	110±8(9)	106±18(17)	89±22(99)	100±18(123)	110±19(208)
			O_3, ppb		
1	62±3(17)	44±13(21)	• • •	23±4(83)	• • •
2	58±11(61)	49±5(402)	40±7(111)	34±12(401)	43±14(411)
3	51±7(49)	49±5(220)	36±11(152)	34±11(109)	49±10(147)
4	52±4(42)	44±8(415)	47±16(134)	27±8(228)	41±7(395)
5	62±14(68)	39±9(212)	50±15(141)	36±10(115)	53±6(252)
6	50±17(60)	38±7(258)	44±9(190)	41±7(330)	50±9(170)
7	53±13(85)	38±6(401)	46±13(418)	44±9(363)	51±13(793)
8	51±8(162)	43±5(232)	45±9(528)	49±9(1170)	55±12(642)
9	45±13(89)	51±11(121)	49±12(519)	54±12(1220)	51±20(1612)
10	57±21(61)	105±19(168)	61±25(478)	56±13(1100)	55±14(1170)

Mean and standard deviation of observed trace gas concentrations in 1985. The number of 7-s ozone and 30-s carbon monoxide observations in each layer is in parentheses.

TABLE 7. Median Mixing Ratios (ppb) of CO and O_3 in Each Equal-Mass Layer and Synoptic Phase of the Meridional Circulation

Layer	P	P(mod)	mT	mT(mod)	Fropa
			CO, ppb		
1	169(146-173)	• • •	• • •	• • •	• • •
2	142(113-168)	144(123-200)	142(120-148)	122(100-165)	178(149-236)
3	149(118-174)	132(110-150)	121(95-137)	120(101-147)	115(96-167)
4	120(104-160)	115(93-143)	131(94-145)	92(82-114)	122(111-131)
5	122(96-154)	94(74-110)	141(122-153)	92(85-111)	130(113-139)
6	113(91-137)	94(73-136)	97(75-125)	88(70-113)	120(110-136)
7	99(91-128)	89(94-99)	98(80-115)	108(90-120)	104(93-126)
8	81(69-109)	91(74-103)	96(83-106)	101(82-118)	112(98-127)
9	69(55-92)	98(90-100)	99(83-117)	109(82-127)	102(84-124)
10	111(93-117)	106(80-131)	86(65-114)	100(83-116)	109(90-129)
			O_3, ppb		
1	61(57-65)	46(21-49)	• • •	24(21-26)	• • •
2	61(44-68)	48(44-53)	41(35-46)	34(22-47)	41(32-58)
3	54(43-58)	49(44-53)	35(24-48)	33(24-48)	51(35-58)
4	53(47-57)	43(37-52)	50(29-63)	27(20-34)	39(34-49)
5	59(48-78)	41(28-47)	53(29-63)	34(28-45)	54(52-56)
6	50(28-67)	39(32-44)	43(36-50)	42(34-46)	53(37-57)
7	56(37-64)	40(31-44)	44(37-51)	46(36-54)	54(36-64)
8	50(42-58)	43(39-47)	46(38-52)	48(41-59)	59(44-65)
9	40(36-55)	48(41-62)	47(38-64)	52(43-66)	58(27-72)
10	46(38-89)	113(85-121)	53(41-84)	55(43-69)	50(40-72)

Median trace gas data, 1985. The range spanned by the first and third quartiles (25% and 75% percentiles) is in parentheses.

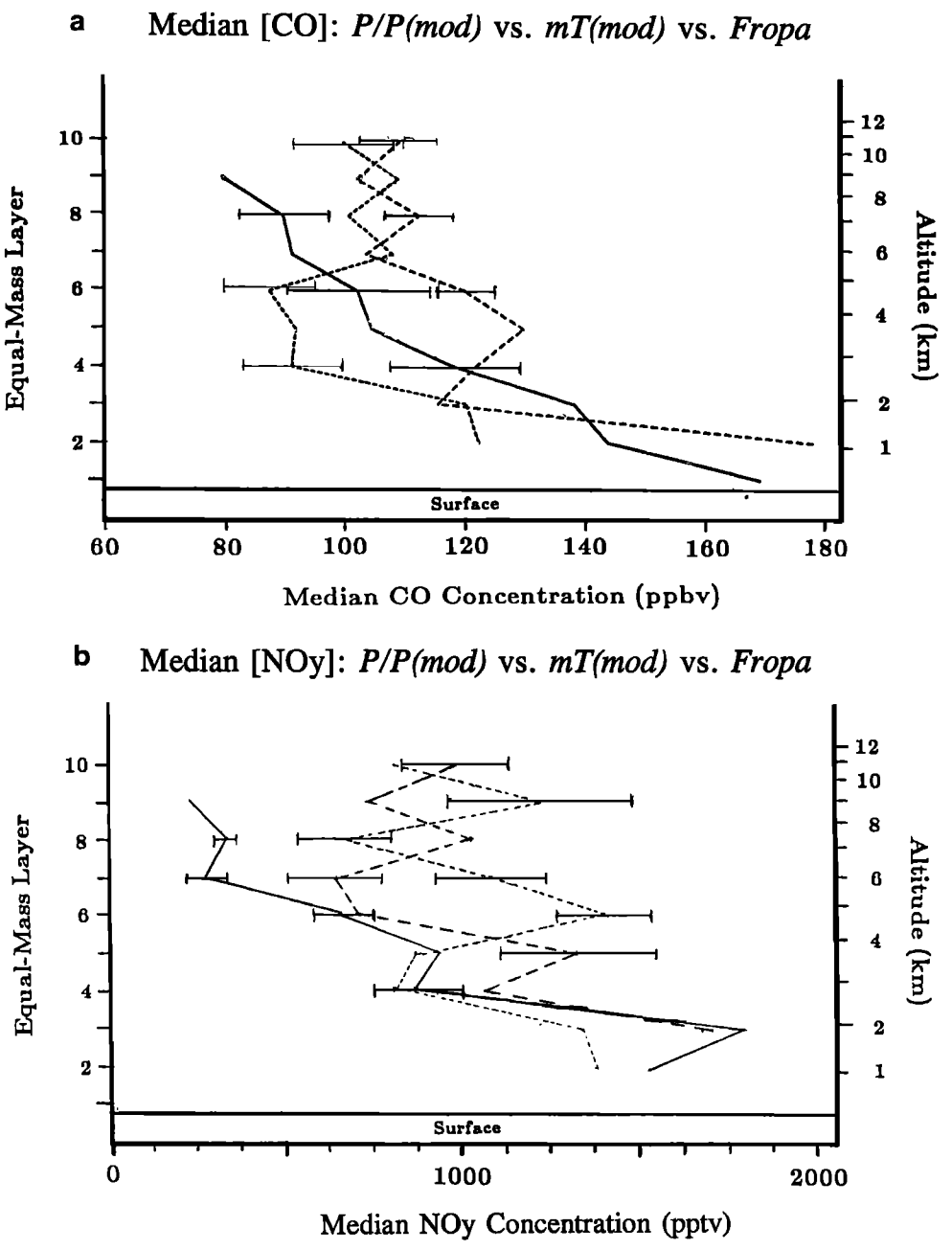

Fig. 2. (*a*) Vertical profiles of CO. Left ordinate is the number of the equal-mass layer, right ordinate is altitude, and abscissa is median [CO] in ppb. The altitude of the Earth's surface above sea-level is indicated by a horizontal line. The solid curve represents data collected in both polar and modified polar flow, P/P(mod); the short dashed curve modified maritime flow; mT(mod), and the long-dashed curve frontal passage fropa. In polar flow, convection is inhibited; in maritime flow, convection tends to transport, planetary boundary layer (PBL) air to the upper troposphere, while near fronts, convection and mixing occur at many levels. Horizontal bars denote a measure of variability within each regime and represent the standard deviation of the observations divided by the square root of the number of flights or flight segments (assumed to be equal to the number of degrees of freedom) within each category; 5 for P/P(mod), 5 for mT(mod), and 7 for fropa; see Table 1). See Tables 6 and 7 for statistics of each layer. (*b*) Same as Figure 2*a*, for total reactive nitrogen, NOy. Note that NOy data are not presented for L2 in fropa flow (polluted PBL) and L10 in P/P(mod) flow (upstream convective activity).

Comparison with other measurements: It would be impractical to compare our observations with previous results on a flight-by-flight basis. In the absence of detailed meteorological observations we make the simplifying assumption that previous trace gas measurements were made largely under clear air, quiescent conditions unaffected by recent convective activity and compare these earlier measurements to our own P and P(mod) data.

We believe this assumption is valid for a variety of reasons. First, most of the trace gas measurements cited in Table 8 were made in the marine environment, or during the winter months (November-February), conditions under which convective

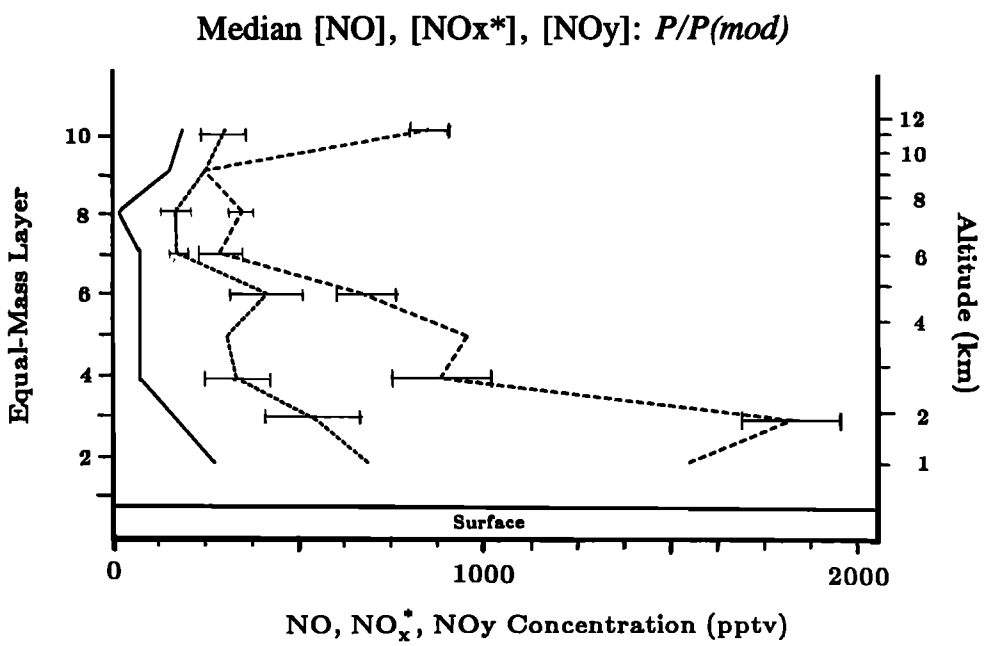

Fig. 3. Vertical profiles of median odd nitrogen mixing ratios for the combined P/P(mod) category; [NO] multiplied by 3 to improve readability. The solid curve represents 3 x [NO], the short-dashed curve [NOx*]; and the long-dashed curve [NOy]. Y axes same as Figure 2. Horizontal bars as in Figure 2. See Tables 4 and 5 for statistics.

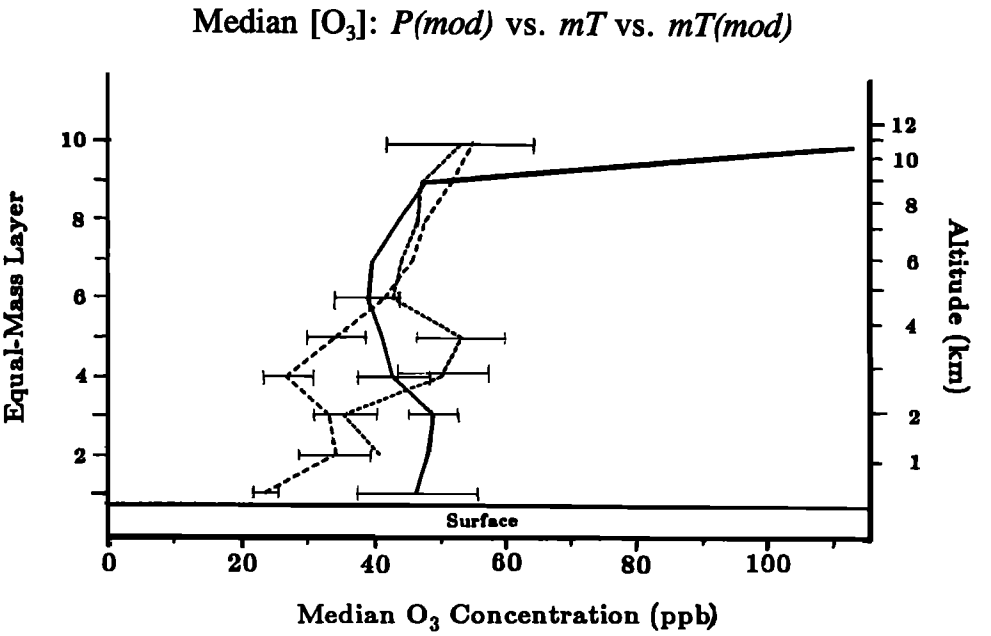

Fig. 4. Profiles of median [O_3]. Solid curve represents data collected in P(mod) flow; the short-dashed line, mT; and the long-dashed line mT(mod). Horizontal bars as in Figure 2. See Tables 6 and 7 for statistics of each layer.

activity can reasonably be expected to be low. In addition, many of the earlier measurements were made in the rural or remote troposphere, where anthropogenic contributions are small. Both considerations require a comparison of the earlier data to our own P/P(mod) observations, which were made in convectively stable flow characteristic of the background troposphere over the flight region. Finally, model calculations of zonally averaged trace gas distributions [e.g., *Logan et al.*, 1981; *Crutzen and Gidel*, 1983] treat vertical trace gas transport via eddy diffusion theory and are comparable only to P/P(mod) data.

Table 8 presents the data from these studies and indicates whether the observations or calculations are similar or dissimilar to those reported here, that is, whether the range of concentrations overlap within experimental uncertainty. Data collected near regions of active convection noted in some previous studies [e.g., *Davis et al.*, 1987; *Ridley et al.*, 1987; *Condon et al.*, 1987; *Torres and Buchan*, 1988] were excluded from further comparison with P/P(mod) results. Finally, data collected in maritime (mT and mT(mod)) or fropa flow will be compared with those literature values clearly applicable to these conditions and are discussed in later sections.

TABLE 8. Comparison With Other Trace Gas Observations

Reference	Altitude Range, km	General Location	Month	Comment
		CO		
Ridley et al. [1990]	4.5-6.1	Continental U.S.	Aug, Sept.	S
Carroll et al. [1990]	0-6.5	Eastern Pacific	Aug.,Sept.	D
	3-6.5	Southwest U.S.	Aug., Sept.	S
Greenberg et al. [1990]	1.5-3	Off California coast	April	S
	6.5-8	Off California coast	April	S
	0-10	Alaska	April	D
Marenco et al. [1989]	1.5-5	East U.S., West Atlantic	June	S
	5-10	East U.S., West Atlantic	June	D
	5-10	Halifax, N.S.; Bermuda	June	S
Van Valin and Luria [1988]	1-4	Bermuda	Feb.-April	S
Condon et al. [1987]	1.5-8	East Pacific,California coast	Nov.	S
Seiler and Fishman [1981]	1-10	U.S. East and West coasts	July, Aug.	S
	>10	U.S. East and West coasts	July, Aug.	D
Heidt et al. [1980]	5.2-6.7	Western U.S.	April, May	S
		NO		
Carrol et al. [1990]	1-6	East Pacific	Aug., Sept.	D
	1-6	Southwest U.S.	Aug., Sept.	S
Torres and Buchan [1988]	2-5	Amazon basin	July, Aug.	D
Fehsenfeld et al. [1988]	2-12	Summary	Varied	S
Drummond et al. [1988]	2-10	East Coast Canada, U.S.	June	S
	Near troposphere	East Coast Canada, U.S.	June	D
Davis et al. [1987]	0-7	East Pacific	Nov.	D
Ridley et al. [1987]	0-7	East Pacific	Nov.	D
Kondo et al. [1987]	3-7	West Pacific	Jan., Feb	S
Logan et al. [1981]	2-11	Zonal average	Summer	S
Model calculation	0-2	Zonal average	Summer	
		NO_x^*		
Gregory et al. [1990]	5	United States	Aug., Sept.	S
Hastie et al. [1988]	0-4	East Coast U.S.	Feb., March	D
Kondo et al. [1987]	3-8	Pacific Ocean	Jan., Feb.	S
	3-8	Industrial Japan	Jan., Feb.	D
Luke and Dickerson [1987]	0-5	Atlantic Ocean	Jan.	S
Dickerson [1984]	9.5	Central Atlantic	Dec.	S
	9.5	East Coast Brazil	Dec.	S
Stedman and McEwan [1983]	SFC (1km asl)	New Zealand remote site	Feb.-May	S
		NO_y		
Hübler et al. [1991]	0-6	Continental U.S.	Aug., Sept.	S
	0-1	East Pacific	Aug., Sept.	D
	1-6	East Pacific	Aug., Sept.	D
Luke and Dickerson [1987]	0-5	East Coast North America	Jan.	S
Crutzen and Gidel [1983]	Lower troposphere	Zonal average	July	D
Model calculation	Midtrop.	Zonal average	July	S
	Upper Trop.	Zonal average	July	D

Under "Comments" S represents similar values to those measured in this study under P/P(mod) conditions, that is, the ranges overlap; D represents dissimilar values.

The CO mixing ratios found in P/P(mod) conditions generally agree with the majority of CO measurements made under nonconvective conditions. The exceptions are data collected in remote maritime areas, such as the eastern Pacific Ocean [*Carroll et al.*, 1990], or downwind of major urban areas, such as the eastern United States [*Marenco et al.*, 1989]. Both *Heidt et al.* [1980] and *Greenberg et al.* [1990] found CO in greater abundance at more northerly latitudes. The concentrations we observed in L10 are 15-20 ppb higher than those reported by *Seiler and Fishman* [1981] at corresponding altitudes, reflecting the importance of upstream convective activity in transporting CO.

Nitric oxide mixing ratios measured in P/P(mod) flow are generally similar to those observed previously in the middle and upper troposphere (see review by *Fehsenfeld et al.* [1988]) but are larger than some observations in remote marine environments [e.g., *Davis et al.*, 1987; *Ridley et al.*, 1987]. On the other hand, NO concentrations in remote areas can be larger if observed in the vicinity of the tropopause or electrically active clouds [*Davis et al.*, 1987; *Drummond et al.*, 1988]. In the planetary boundary layer (PBL) the NO concentrations reported here are consistently higher than values obtained in remote locations. Our measured NO concentrations in the middle and upper troposphere agree reasonably well with model-calculated

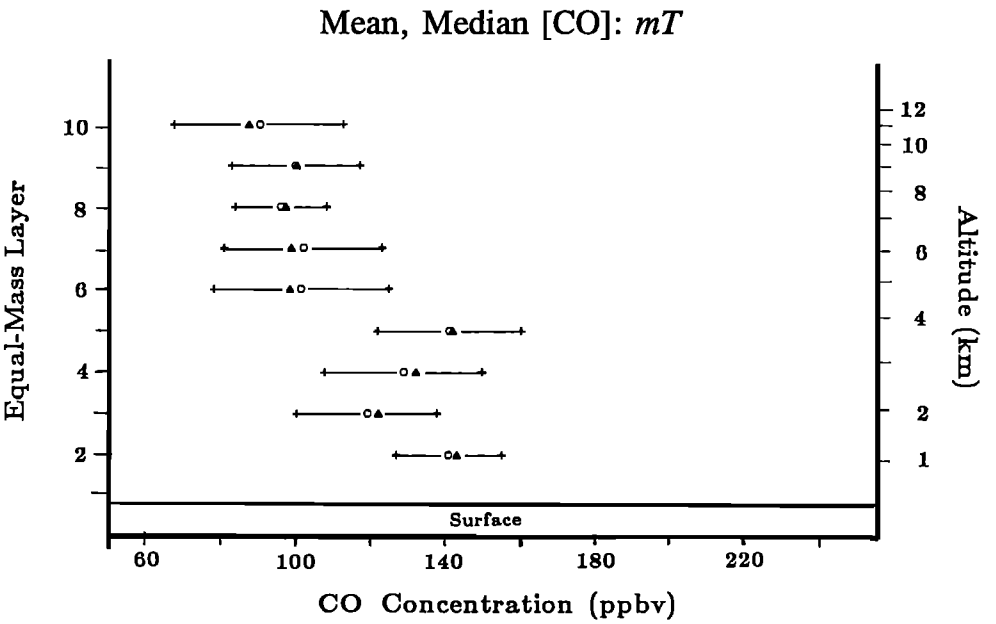

Fig. 5. Profiles of [CO] for the mT flow category; circles represent the mean; triangles, the median; and bars, the standard deviation of 30-s averages in each layer. See Tables 6 and 7 for statistics.

concentrations (at 45°N under clear sky conditions in summer) [*Logan et al.*, 1981]. In the lower troposphere, where regional emissions are important, measurements show much more NO than the zonally averaged model predictions.

The NO_x* concentrations we observed in the free troposphere (FT) are similar to previous measurements using a $FeSO_4$ converter (Table 8), except those clearly affected by industrialized centers. For example, our concentrations are somewhat smaller than those measured over industrialized Japan [*Kondo et al.*, 1987] and off the American East Coast [*Hastie et al.*, 1988].

Our NO_y measurements are similar to those recently made in the PBL and FT over the continental United States and in the FT over the eastern Pacific but are considerably larger than concentrations encountered in the marine boundary layer [*Hübler et al.*, 1992]. We can also compare our observations to model calculations [*Crutzen and Gidel*, 1983]. The NO_y mixing ratios measured in the lower troposphere are quite a bit higher than the predicted 200 to 400 ppt, probably due to zonal averaging of industrial emissions. In the highest layer, L10, upstream convective activity increased NO_y mixing ratios above model predictions [see *Pickering et al.*, 1989]. In the midtroposphere, however, observations and model calculations are in much better agreement.

Maritime tropical flow (mT). As noted in part 1, mT air is characterized by moist, southerly flow from the surface through 850 mbar which transports air from the densely populated and heavily industrialized Gulf Coast into the flight region. Conditional instability through a deep layer creates conditions favorable to the efficient and rapid transport of these emissions to the FT over a wide geographical area [*Mc-Namara*, 1988; *Ryan*, 1990; *Ryan et al.*, this issue]. To observe the magnitude of this effect, compare the CO profile observed under *mT* conditions with that observed under P/P(mod) conditions (Figures 5 and 2); likewise, compare the NO_x* profiles (Figures 6 and 3).

The mT branch of the meridional circulation is heavily represented by data collected on flights R12 and R13 (June 22, 1985), shortly after a "hybrid" mesoscale convective system (MCS) developed over the flight region [*Bartels et al.*, 1984; *McNamara*, 1988; *Ryan*, 1990; *Pickering et al.*, 1990]; we will briefly describe the effects of the mesoscale dynamics upon the observed trace gas profiles. Upon takeoff, surface winds were southerly at 180°, and the outbound leg of R12 sampled fairly clean air as the Sabreliner climbed through a broken stratocumulus deck associated with the remnants of the MCS [*Ryan*, 1990]. The average ozone concentration in L4 during this period was 34 ppb. Later in the flight, the high-pressure center situated to the southeast regressed slightly westward. Winds near the surface backed to 160°, advecting moist air from the Gulf of Mexico over the Texas and Louisiana coasts and into the flight region. The return leg of R12 reflected the presence of this deep, polluted layer; average ozone concentrations in L4 increased to 58 ppb. (The low median $[O_3]$ in L3 (~35 ppb; see Figure 4) reflects the large influence of the generally low ozone mixing ratios measured on flight R15.) The mixed layer deepened during R13 and extended as high as 650 mbar. This layer was capped by fair weather cumulus clouds in the flight region [*McNamara*, 1988; *Ryan*, 1990], and ozone concentrations in L4 remained at 58 ppb. Carbon monoxide and NO_x* profiles (Figures 5 and 6) also reflect the presence of the deep, well-demarcated impulse of polluted Gulf air. Neither CO nor odd nitrogen data were collected on the outbound (clean air) leg of R12, however.

The influence of anthropogenic emissions in the polluted air mass from the Gulf may be demonstrated by comparing our trace gas data to previous measurements made in the area. *Heikes et al.* [1987] measured ozone upwind of the major emission sources along the Gulf Coast and reported concentrations of 35 ppb at 3.3 km (that is, L4) in November. This concentration agrees well with levels we measured in the MCS remnants but is 20-25 ppb lower than those we encountered in the polluted air of the Gulf; the larger concentrations reported here reflect both the regional photooxidation of enhanced ozone precursors and increased photochemical activity in the summer months. Our measurements in polluted Gulf air agree well with

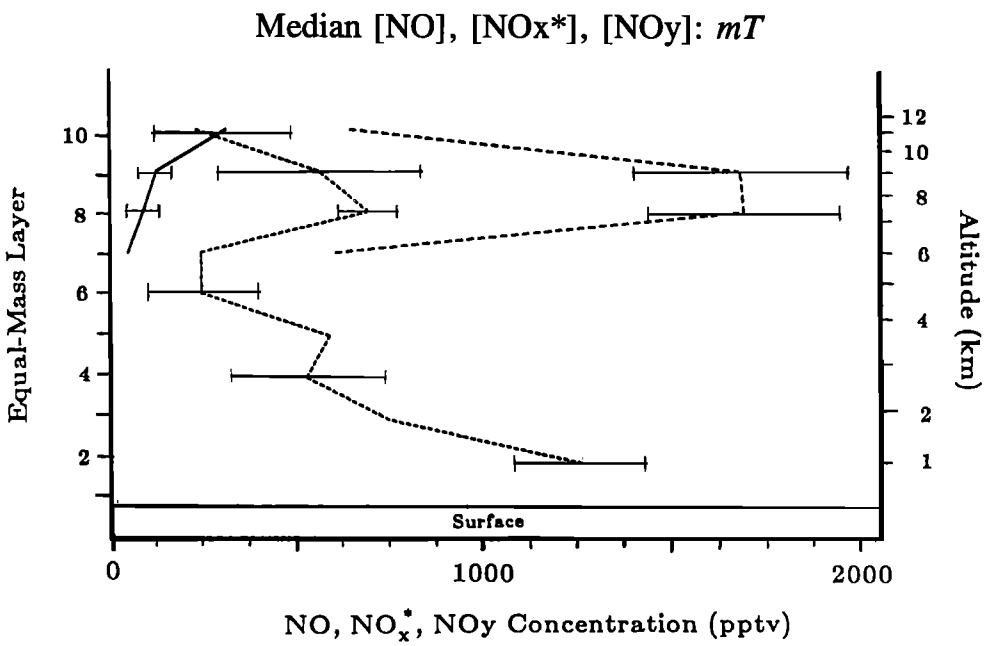

Fig. 6. Profiles of odd nitrogen for the mT category. The solid curve represents median [NO] (not multiplied by 3); the short-dashed curve [NOx*]; and the long-dashed line, [NOy]. Horizontal bars as in Figure 2. See Tables 4 and 5 for statistics.

those of *Boatman et al.* [1989], who reported summertime O_3 concentrations of 63 ±10 ppb and 61 ±7 ppb at 1450 and 2450 m, respectively, under similar conditions. Overall, however, O_3 concentrations encountered in the lower troposphere during mT flow (Table 7) are smaller than summertime ozone concentrations measured over more polluted areas in the northeastern United States [*Boatman et al.*, 1990; *Van Valin et al.*, 1990].

Carbon monoxide data may be used to examine the differences in vertical transport between maritime and polar flow conditions. Convective instability in maritime flow deepens the mixed layer and enhances trace gas concentrations throughout; median [CO] reaches a local maximum (141 ppb) in L5 before decreasing to 97 ppb in L6 (Figure 5). This deep mixed layer contrasts with the shallow PBL observed in subsiding polar flow, where median CO concentrations drop dramatically above L3.

In the middle and upper middle troposphere (L6-L8), median [CO] in mT flow is only 3 to 9 ppb larger than corresponding levels encountered under P(mod) conditions (Table 7). The fair weather cumulus clouds capping the mixed layer on R13 extended to a maximum altitude of only 4.5 km and lacked sufficient vertical development to transport polluted air from the PBL to the upper troposphere. Thus the enhanced trace gas concentrations observed in the PBL are not seen in the free troposphere. Instead, the weak concentration gradients of O_3 (Figure 4) and CO (Figure 5) from L6-L10 reflect the convective overturning of the earlier MCS which decayed over the flight region [*Ryan et al.*, this issue].

Carbon monoxide data collected under mT flow are in substantive agreement with previous measurements. Our mean CO concentrations in L2 and L3 (140 ±14 ppb and 118 ±19 ppb, respectively) agree well with that measured under maritime flow by *Boatman et al.* [1989] (117 ±26 ppb at 1450 m, the top of L2). Our mean [CO] in L4 (128 ±21 ppb), however, is significantly larger than that measured by Boatman et al. (88 ±15 ppb at 2450 m), who presumably did not encounter a deep mixed layer.

Median odd nitrogen concentrations observed under mT flow are illustrated in Figure 6. The local maximum of [NO_x*] in L5 corresponds to the maxima in median [CO] and [O_3] observed there. Both the mean concentration and standard deviation of NO_x* (Table 4) fall in L6 and L7, then increase in L8-L10, reflecting the recent injection of these trace gases in the outflow regions of the convective storms [e.g., *Junge*, 1974]. Median NO increases from 50 ppt in L7 to 312 ppt in L10. The lack of a significant increase of CO in the upper troposphere during *mT* flow suggests that lightning is largely responsible for the observed enhancement of odd nitrogen [e.g., *Chameides et al.*, 1977; *Borucki and Chameides*, 1984; *Chameides et al.*, 1987*b*; *Davis et al.*, 1987; *Ridley et al.*, 1987; *Torres and Buchan*, 1988; *Dye et al.*, 1989] and may lead to the formation of photochemical "hot spots" in the anvils of the electrically active clouds [e.g., *Chameides et al.*, 1987*a*]. This topic will be further discussed in a later section.

It is interesting to note that the enhancement of NO in the upper troposphere in mT flow may be large enough to transform the region from one of net photochemical ozone destruction to one of net ozone production. For example, median [NO] in L8 jumped from 3 ppt under P/P(mod) conditions to 93 ppt in mT flow.

Daum et al. [1990] measured NO_y in the vicinity of thunderstorms over Ohio during summer. Their results agree well with ours in the lower troposphere (L2-L4), but not at higher altitudes, where they report 0 to 350 ppt at 625 mbar (L6). The discrepancy may be related to the 0.2 ppb detection limit of their instrument.

Modified Maritime Flow (mT(mod)). The dry capping layer at 900-700 mbar which characterizes mT(mod) flow [*Carlson et al.*, 1983; *Ryan et al.*, this issue] may suppress widespread midday convection in the flight region but often sets the stage for deep, locally focused convective activity that can grow overnight to enormous size. Intense solar heating forces isolated air parcels through the dry cap where they quickly accelerate upward in the unstable environment [e.g., *Carlson and Ludlam*,

1968; *Anthes et al.*, 1982; *Carlson et al.*, 1983]. The presence of the capping inversion thus induces intense convective behavior which is reflected in the vertical redistribution of trace gases over the flight region.

Whereas CO concentrations are enhanced up to an altitude of 4 km (L5) in the deep mixed layer associated with mT flow, CO levels in mT(mod) flow decrease sharply from ~120 ppb in L3 to ~90 ppb in L4-L6 (compare Figures 2 and 5). Carbon monoxide concentrations in the lower to midtroposphere (L2-L6) under mT (mod) conditions are even smaller than corresponding concentrations observed in P/P(mod) flow (Figure 2). In the upper troposphere, however, median mT(mod) [CO] increases to 108 ppb in L7 and remains quite high through L10, reflecting the efficient vertical transport of polluted boundary layer air. This deep convection may be contrasted with conditions encountered in mT flow, where shallow cloud vertical development precluded significant transport of polluted Gulf air to the upper troposphere.

Figure 7 shows vertical profiles of NO, NO_x*, and NO_y observed in mT(mod) flow. Layers 2-7 of these profiles resemble observations made in polar airflow (Figure 3), with low absolute concentrations and little variability (Table 5). In L8-L10, however, both the concentration and variability of NO and NO_x* increase dramatically (Figure 2*b*). For example, NO_y is enhanced over P/P(mod) levels in L6 and above (Figure 2*b*). Mean [NO] in L8 is 231 ppt, yet the median concentration is only 28 ppt. This increase in NO is not accompanied by a correspondingly large increase of [CO], implicating lightning as the primary source of odd nitrogen.

The median ozone profile for mT(mod) flow, depicted by the long-dashed curve in Figure 4, shows concentrations in L2-L5 smaller than corresponding mT and P(mod) concentrations; in fact the mT(mod) data constitute the lowest ozone levels at these altitudes for all phases of the meridional exchange. In the upper troposphere, however, ozone concentrations in mT (mod) flow are larger than corresponding mT and P(mod) concentrations, excluding values directly affected by the stratosphere. The increases in upper tropospheric CO and odd nitrogen under mT(mod) conditions, unaccompanied by similar increases in O_3, suggest only recent injection of boundary layer air and insufficient time for photochemical ozone production.

Trace gas concentrations can be used to illustrate another aspect of the cloud dynamics characteristic of mT(mod) conditions: the absence of detrainment of PBL air in the midtroposphere. As discussed above, mT(mod) concentrations of CO and NO_x* in L4-L6 resemble the low levels encountered in the P(mod) regime and are significantly lower than corresponding levels observed in mT flow. As noted in part 1, midtropospheric horizontal back trajectories for mT(mod) and mT flow are very similar. We thus attribute the observed differences in trace gas concentrations to the more intense convective activity observed in mT(mod) flow. While mT flow is characterized by a deep mixed layer of polluted air, the capping layer of mT(mod) flow confines the mixed layer closer to the surface and inhibits small-scale convection. Once an air parcel breaks through the cap, however, convection is violent and deep. Detrainment under these conditions (at least for the growing or mature stages when we sampled) occurs primarily in the upper troposphere, leaving the midtroposphere relatively clean. Observations of cloud type and amount, summarized in part 1, bear out this hypothesis: almost all mT(mod) cases were characterized by cumulonimbus clouds extending from altitudes of 6-10 km. Our observations are also consistent with the results of a modeling study of an MCS over Africa in which low-level air ($z \leq 2$ km) detrained mainly above 6 km (that is, L7) [*Moncrieff*, 1989]. Similar results have been demonstrated by *Pickering et al.* [1991] from a model simulation of a squall line over the Amazon basin in the dry season.

Frontal passage (fropa). Frontal passage provides the transition between polar and maritime air masses in the flight region. Overrunning mT air produces stratiform clouds as air parcels are convectively forced at many levels along the front. Convective cells may be embedded in these stratiform layers. It is important to remember that the classification of fropa flow

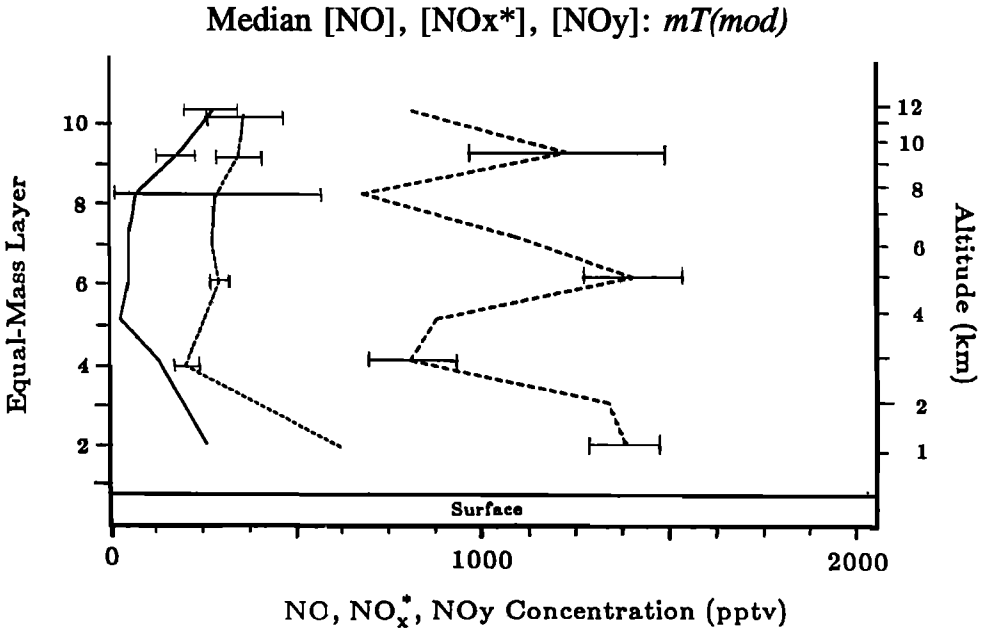

Fig. 7. Profiles of median odd nitrogen mixing ratios for mT(mod) category; [NO] multiplied by 3 to improve readability. The solid curve represents 3 x [NO]; the short-dashed line, [NOx*]; and the long-dashed line, [NOy]. Horizontal bars as in Figure 2. See Tables 4 and 5 for statistics.

was designed not to locate the position of the cold (or stationary) front itself but rather to identify air that had been processed by convection associated with the front. At high altitudes the first encounter with a cirrus, cirrostratus, or altostratus deck marks the upper level edge of air associated with the front. These clouds are believed to result from forced ascent in the vicinity of the frontal zone and have been blown east, ahead of the front, by the strong upper level winds. At low levels, air processed by convection along the frontal zone is marked by a transition from clear (cloud free) conditions to deep or well-developed cumulus clouds north or west of the analyzed surface front [*Ryan*, 1990; *Ryan et al.*, this issue].

The ascent of overrunning maritime air and embedded convection under fropa conditions modify the sharp [CO] gradient characteristic of P/P(mod) flow (Figure 2*a*). Median CO concentrations in fropa flow are larger than those observed in P(mod) flow in nearly all layers (Table 7). The degree of enhancement ranges from 3 ppb in L10 to 36 ppb in L5. Large CO concentrations were observed in the PBL in the urban plume advected well downwind of Oklahoma City. Thus although the effects of local urban pollution were systematically removed from the PRECP data set [*Ryan*, 1990; *Ryan et al.*, this issue], isolated episodes of urban contamination are unavoidable and indeed representative of conditions occasionally encountered in the flight region.

The vertical profile of median [CO] observed in fropa flow (Figure 2*a*) suggests that the broad, layered lifting which accompanies frontal passage overturns large portions of the troposphere along the line of convection, efficiently mixing the troposphere at a variety of levels. In the upper troposphere (L7-L10), median [CO] during frontal passage resembles concentrations observed in the outflow regions of the deep convection of mT(mod) flow. Unlike mT(mod) flow, however, CO concentrations in the middle troposphere (L4-L6) are also enhanced during frontal passage. Thus although frontal zones may effectively cap the polluted PBL and suppress the transport of pollutants to the upper troposphere [*Pickering et al.*, 1988], the bulk effect of frontal passage is to mix [CO] uniformly from the surface to the upper troposphere. Because the lifetime of tropospheric CO is of the order of a few months [*Thompson and Cicerone*, 1986], the uniform vertical CO profiles do not necessarily result from convection in the immediate flight vicinity but may result from the cumulative effects of upstream convective activity along the advancing frontal zones. An examination of fropa ozone concentrations (below), as well as cloud observations presented in part 1, suggests that this is indeed the case. While most of the fropa cases encountered stratiform and convective clouds at altitudes of 6-10 km, two of the seven cases encountered clouds at almost all levels in the troposphere. Upstream convective activity within the previous 5 hours was documented in six of the seven flight segments (see part 1).

Vertical [CO] gradients (in ppb CO/100 mbar) were calculated for each branch of the meridional circulation from the median [CO] and atmospheric pressure at the midpoint of each equalmass layer (Table 9). Note that in none of the categories do median CO concentrations increase with altitude when all layers are considered. The correlations help to quantify the flattening of the concentration gradient in the presence of convective transport.

For the fropa case, profiles of NO, NO_x*, and NO_y (Figure 8) exhibit similar shapes, with smoothly decreasing concentrations above L2, a local minimum in L6 or L7, and larger concentrations above (Figure 2b). The lifetimes of odd nitrogen species in the troposphere are of the order of days, so their profiles should reflect more recent vertical transport near the flight region. The increase in both odd nitrogen concentrations and their coefficients of variability suggest that the primary level of detrainment over the flight region itself lies above 5 km, consistent with observations of cloud type presented in part 1.

TABLE 9. Carbon Monoxide Gradients Observed in Each Branch and Sub-Phase of the Meridional Circulation

	Carbon Monoxide Gradients		
Category	Gradient ppb CO/100 mbar	r	Layer Included
Polar	14	0.98	L1-L9
P(mod)	12	0.92	L2-L8
mT	8.2	0.85	L2-L10
mT(mod)	1.8	0.33	L2-L10
Fropa	3.1	0.65	L3-L10

Gradients were calculated from the median [CO] and the pressure (mbar) at the midpoint of the layers noted. Small case "r" represents correlation coefficients for CO and altitude layer.

Odd nitrogen concentrations under fropa conditions, especially in the upper troposphere, are typically lower and less variable than under mT conditions, but CO concentrations are larger (Tables 5 and 7). This suggests that transport, not electrical activity, plays the dominant role in enhancing upper tropospheric NO during frontal passage. With the exception of L7 and L9, median NO concentrations are enhanced in all layers relative to combined polar flow categories; the median concentration in L8 (109 ppt) is much larger than in polar flow (3 ppt). Median NO_y concentrations are similarly enhanced over P/P(mod) levels (Figure 2b).

The profiles of O_3 in the FT during frontal passage (Figure 9) show high median mixing ratios (around 50 ppb) and little variation with altitude, although the variation within each altitude layer is substantial. Ozone concentrations in the upper troposphere are generally larger than under mT(mod) flow, but CO levels are similar. We initially suspected the increased fropa O_3 concentrations to have resulted from tropopause "folding" events, in which tongues of stratospheric air descend into the middle and upper troposphere. These events are frequently observed in the mid-latitudes [*Danielsen et al.*, 1968] and are associated with complex circulations that accompany accelerations ("jet streaks") in the jet stream. In addition, such intrusions are often coincident with frontal zones. For the frontal passage flights, however, no nearby jet streaks are analyzed in the NWS 200- and 300-mbar constant pressure charts. Tropopause heights, as determined by OKC rawinsonde data in the wake of the fronts, were quite high (120-160 mbar) so that small-scale mixing of stratospheric air was unlikely. Finally, large variations in θ and θ_e would be expected when pockets of stratospheric air mixed downward due to penetration of the tropopause by thunderstorms. The Sabreliner data show no such variation, however, and we conclude that stratospheric intrusions were not responsible for the enhanced ozone concentrations.

To determine the origin of the increased and variable O_3 concentrations observed in the upper troposphere (L9 and L10) under fropa conditions, we analyzed ten events of high ($\geq$ 55 ppb) and low ($<$ 55 ppb) O_3 concentrations for the seven

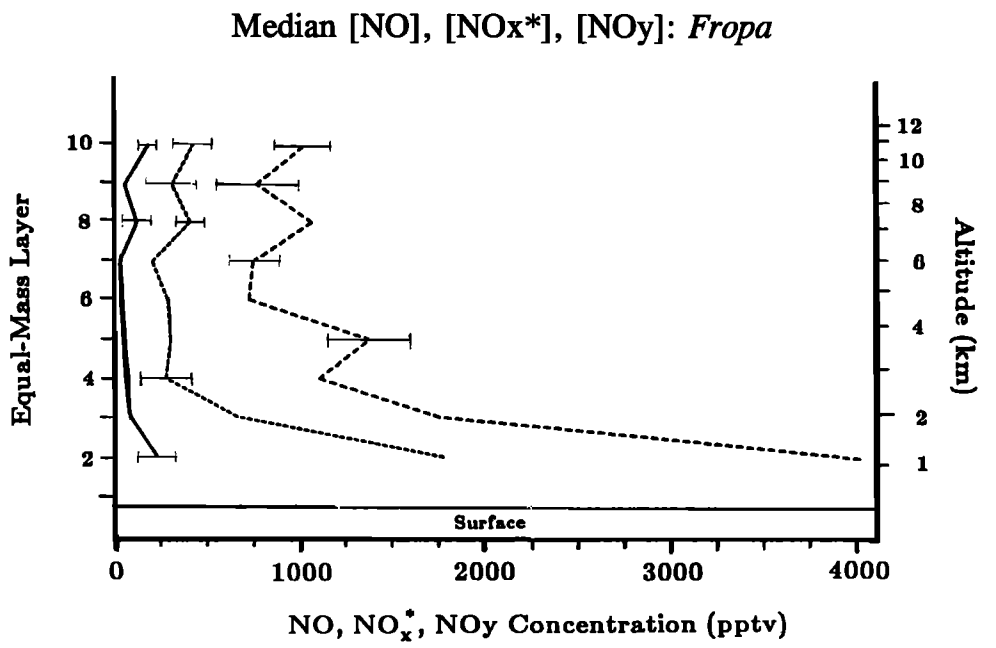

Fig. 8. Profiles of odd nitrogen for fropa flow; solid curve represents median, [NO] (not multiplied by 3); short-dashed line, [NOx*]; and long-dashed line, [NOy]. Horizontal bars as in Figure 2. See Tables 4 and 5 for statistics.

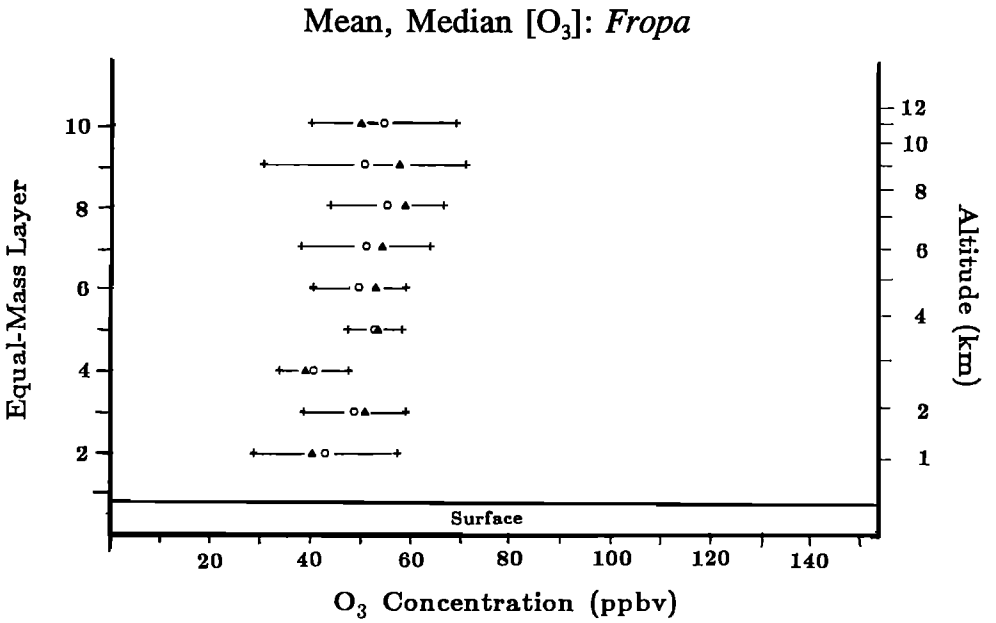

Fig. 9. Profiles of [O_3] for the fropa flow category; circles represent the mean; triangles, the median; and bars the standard deviation of 30-s averages in each layer. See Tables 6 and 7 for statistics.

research flights which constitute the fropa category. The low O_3 values were measured on three flights (R9, R15, R16), while high O_3 values were encountered on four (R1, R8B, R10, R17).

Several factors can explain the low ozone concentrations observed on flights R9, R15, and R16. In R9, for example, entrainment of air from midlevels, above the frontal zone and PBL, resulted in low ozone concentrations [*Pickering et al.*, 1988]. In R15 and R16, however, the flights investigated growing convective cells over the leading edge of the frontal zone (just north of the surface frontal position). These cells were located to the south and west (upstream) of previous events. Unlike R9, these thunderstorms appeared to be entraining PBL air, as evidenced by high CO concentrations. Ozone remained low, however, as there was little time for photochemical production to take place. The flight path of R16 was initially on the southern periphery (upwind) of the growing cells and O_3 concentrations were low. When the aircraft left this cell to sample farther north of the frontal zone, it passed through cirrus clouds associated with a preexisting thunderstorm. As the Sabreliner penetrated the cirrus veil, ozone concentrations increased sharply.

In most of the high-[O_3] flights the Sabreliner sampled air which had been repeatedly disturbed by convective activity associated with the advancing front. In three of the four high-[O_3] flights (R8B, R10 and R17) the flight path covered areas to the west and north of frontal zones in which deep convection,

as seen in satellite images, had been occurring for at least 7 hours prior to the flights. As a result, there was sufficient time for photochemical O_3 production from transported precursors to take place [e.g., *Chameides et al.*, 1987; *Pickering et al.*, 1990]. The high ozone values encountered in the remaining flight (R1) do not follow the pattern seen above. Although this flight was in a region in which convection had been occurring for some time, the high ozone levels were associated with a thin (100 mb thick), inhomogeneous layer of air advected from the northwest and embedded in upper and lower level flow from the southwest. In general, however, the degree of previously occurring, upstream convection is strongly correlated with extremes in high-altitude [O_3], and reconciles the vertical profiles of CO, odd nitrogen, and O_3 in fropa flow.

Trace gas concentrations recorded during frontal passage provide compelling observational evidence that convective transport of ozone precursors and their subsequent photochemical reactions can significantly increase ozone in the upper troposphere at locations well downstream of the initial convection. Presumably, increased ozone concentrations would be observed downstream of the outflow regions of the maritime convective storms as well.

3.2 *Trace Gas Histograms*

The analysis of vertical profiles of trace species and the variability of their concentrations provide an estimate of the degree of enhancement over background concentrations induced by both the vertical instability and the recent horizontal trajectories of maritime and fropa flow. However, trace gas histograms provide a more complete demonstration of the population statistics and range of concentrations encountered in each phase of the circulation and thus should be of use in computer models of tropospheric chemistry. Histograms can also provide important insights into the origins and histories of the sampled air masses, insights which may be obscured by a consideration of mean and median profiles alone. Uniform, well-mixed air parcels would be expected to display homogeneous, narrow frequency distributions of trace gas concentrations, while parcels characterized by a multitude of different source regions or histories should exhibit structured distributions.

Frequency distributions of data collected in each branch of the meridional circulation are presented below. Data collected in P and P(mod) conditions were combined to represent typical trace gas distributions in the postfrontal environment; mT and mT(mod) data were combined to reflect the range of concentrations encountered in the warm sector ahead of surface cold fronts. In order to conveniently illustrate the effects of synoptic flow on the vertical distribution of tropospheric trace gases we constructed histograms for nearly constant volume fractions of the troposphere: (1) the lower troposphere, extending from 0 to 4.17 km and encompassing L1-L5; (2) the middle troposphere, extending from 4.17 to 7.98 km and incorporating data in L6-L8; and (3) the upper troposphere, extending from 7.98 to 12.01 km and including data collected in L9 and L10. Trace gas data were binned into the appropriate concentration interval (5 ppb for O_3, 10 ppb for CO, 25 ppt for NO, and 100 ppt for NO_y). Measured concentrations below the detection limit of the instruments were placed in the first concentration interval. The resulting histograms were then normalized to the largest number of observations in any concentration interval within the distribution.

Lower troposphere. Frequency distributions of [CO] in the lower troposphere are illustrated in Figure 10. The distribution observed under polar flow conditions reflects the superposition of polluted plumes, which retain much of their initial identity in the convectively stable flow, upon cleaner background air. Concentrations less than 110 ppb characterize extremely clean P and P(mod) air, while those at 120-130 ppb typify the FT in the P regime. Observations of [CO] > 130 ppb denote varying

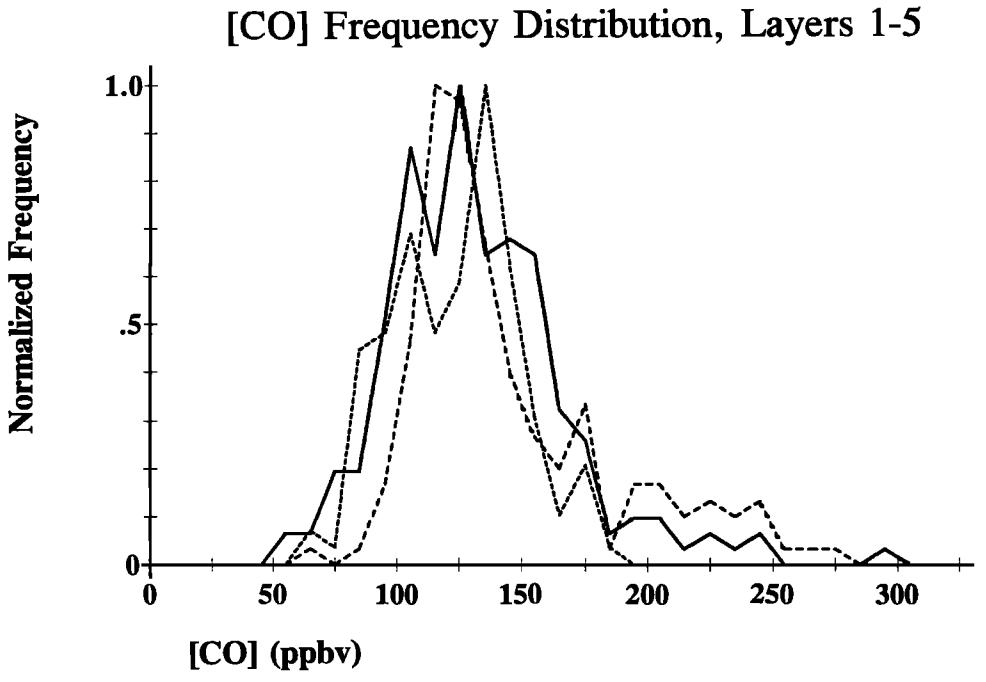

Fig. 10. Normalized frequency distributions of [CO] in the lower troposphere (L1-L5; 0-4.17 km). Solid curve depicts observations in P/P(mod) flow; short-dashed line, mT/mT(mod); and long-dashed line, fropa. The width of each concentration bin is 10 ppb. The number of observations in each bin is normalized to the largest number of observations in any one bin.

degrees of pollution. Data collected in maritime flow display a wide range of concentrations. Incursions of polluted Gulf air in mT flow give rise to CO concentrations of 130-140 ppb in the lower troposphere. In mT(mod) flow, however, concentrations of 70-110 ppb are recorded in the clean, dry air of the lower FT as well as in the downdrafts of intense convective storms. The uniform distribution of fropa flow peaks at 110-120 ppb and suggests a well-mixed lower atmosphere. Carbon monoxide concentrations less than 100 ppb are rarely observed in fropa flow, in contrast to polar and maritime conditions which frequently give rise to such concentrations.

The narrow, uniform [O_3] frequency distribution observed during episodes of polar flow (Figure 11) stands in sharp contrast to the structured CO frequency distribution observed there and suggests little history of recent photochemical ozone production. Although sufficient concentrations of odd nitrogen exist to ensure some degree of photochemical production in almost all layers, the possibly rapid depletion of reactive NMHCs in the aged, clean air may limit photochemical ozone production to that from the relatively slow oxidation of carbon monoxide and methane [e.g., *Liu et al.*, 1987; *Trainer et al.*, 1987]. Unfortunately, no NMHC data with which to evaluate this hypothesis were collected in either P or P(mod) flow. The histogram of ozone data collected in maritime flow, like that of carbon monoxide, illustrates the varying levels of pollution found in the lower troposphere under these conditions. Ozone concentrations in the lower troposphere peak at 45-50 ppb in polluted mT flow from the Gulf and at 20-25 ppb in cleaner mT(mod) flow. The bimodality of the fropa O_3 histogram contrasts with the homogeneity of the fropa [CO] histogram. This bimodality does not reflect [O_3] differences between the polar air below the front and the overrunning maritime flow, as these phases of the meridional circulation display similar concentrations. Instead, fropa O_3 concentrations of 35-40 ppb characterize air only recently processed by convection along the front, while concentrations of 50-55 ppb denote enhanced photochemical production in air repeatedly disturbed by convection.

Middle troposphere. Normalized frequency distributions of CO data collected in the middle troposphere are illustrated in Figure 12. As in the lower troposphere, the structured distribution of [CO] under polar flow suggests the superposition of polluted plumes ([CO] > 130 ppb) upon broad areas of clean air (100 ppb > [CO] > 70 ppb). The maritime [CO] distribution displays the same mode observed in polar flow (90-100 ppb), indicating that the deep impulses of Gulf air characteristic of strong mT episodes and the organized convection common to mT(mod) flow leave the middle troposphere largely undisturbed. Finally, the fropa distribution peaks at CO concentrations about 10 ppb higher and displays appreciably more observations above 120 ppb than either polar or maritime flow. The homogeneity of the fropa distribution suggests that the thorough mixing inferred in the lower troposphere extends to middle levels as well.

Histograms of ozone data collected in the middle troposphere (Figure 13) mimic the distributions of CO at these altitudes. The relatively narrow frequency distribution of polar [O_3] data probably reflects the slow photochemical production in the middle troposphere during episodes of polar flow. Maritime ozone concentrations are somewhat more broadly distributed than polar values, but the mode of the distribution is similar to that observed in polar flow. The fropa ozone distribution peaks at 60-65 ppb and exhibits much larger concentrations than either polar or maritime flow. This degree of enhancement is much larger than that of carbon monoxide and suggests photochemical production from precursors injected aloft by upstream convection along the front.

Upper troposphere. The histograms of CO data collected in the upper troposphere are illustrated in Figure 14. In polar flow, CO concentrations of 60-70 ppb characterize air well behind the sloping isentropic surfaces of the cold front. Concentrations of 130-140 ppb were observed on R5 in the

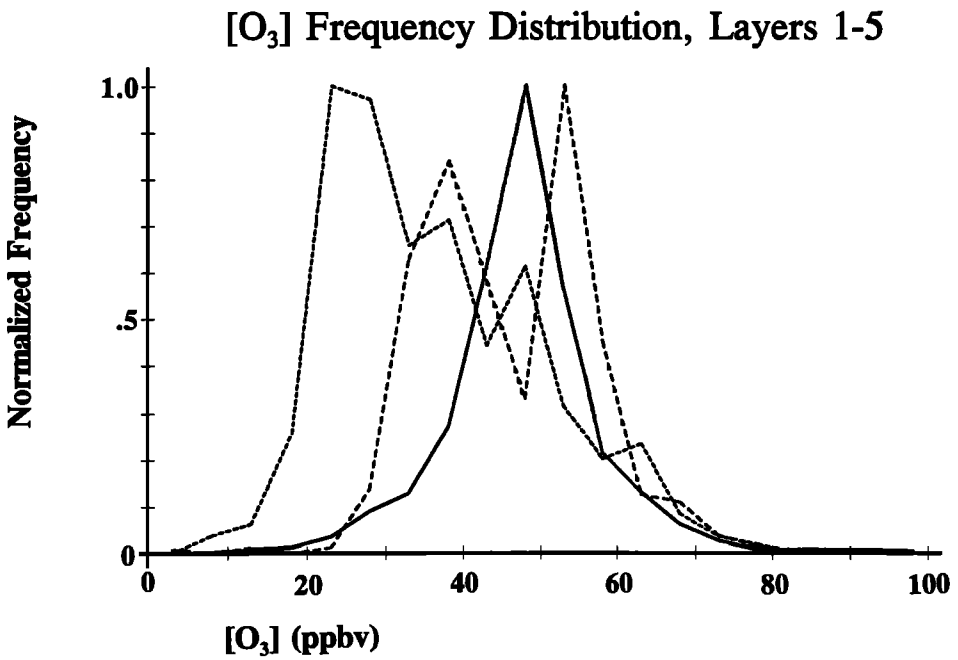

Fig. 11. Normalized frequency distributions of [O_3] in the lower troposphere. Solid curve depicts observations in P/P(mod) flow, short-dashed curve mT/mT(mod); and long-dashed line, fropa. The width of each concentration bin is 5 ppb.

polluted urban plume injected into the upper troposphere by upstream convective activity [*Pickering et al.*, 1989]. In maritime flow the enhancement of CO in the upper troposphere by organized mesoscale convective activity ([CO] = 110-130 ppb) is typically observed in PBL air mixed upward and injected into the clean background air of the upper troposphere ([CO] ≤100 ppb). The homogeneity of the fropa [CO] distribution again attests to the efficient mixing resulting from frontal passage; the distribution peaks at 90-110 ppb and displays consistently larger CO concentrations than either polar or maritime flow.

Cloud electrical activity dominates the high end of the NO frequency distributions in the upper troposphere (Figure 15). Nitric oxide concentrations encountered in maritime flow often ranged from 300 to 1200 ppt, while those measured during frontal passage never exceeded 600 ppt. Nitric oxide concentrations in polar flow never exceeded 225 ppt and rarely exceeded 125 ppt. The pattern is much the same in the middle troposphere (not shown), where the single highest [NO], 4.1 ppb, was observed in maritime flow. If convective transport were responsible for the significant enhancement of NO in the middle and upper troposphere under maritime conditions, then CO should be enhanced to a similar degree; however, levels of CO in maritime and polar flow are roughly comparable (Figure 12).

Upper tropospheric distributions of [NO_y] (Figure 16) also reflect the importance of lightning in maritime flow. The

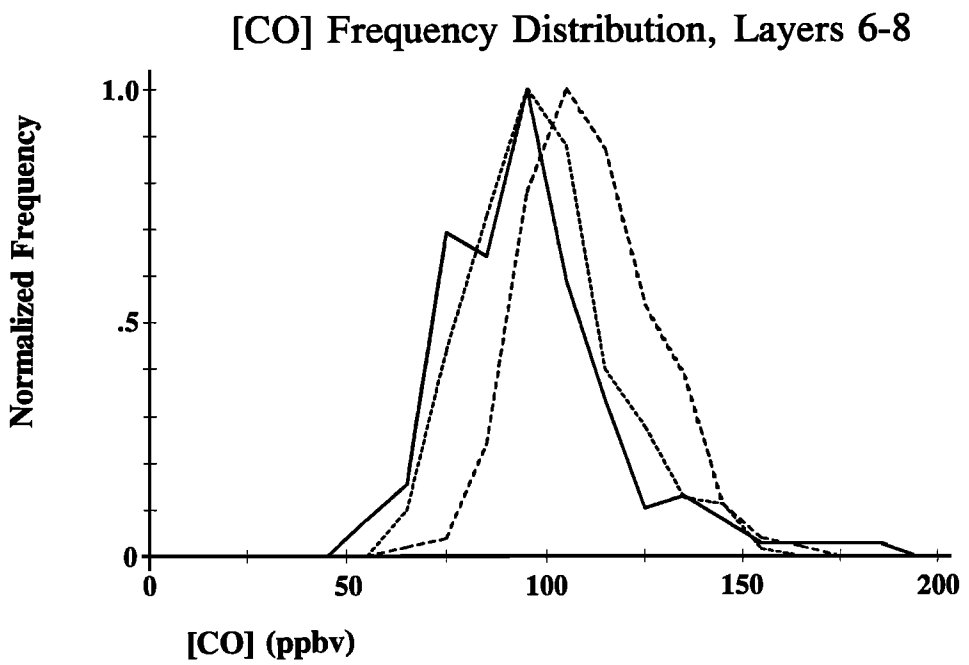

Fig. 12. Same as Figure 10, for the middle troposphere (L6-L8; 4.18-7.98 km).

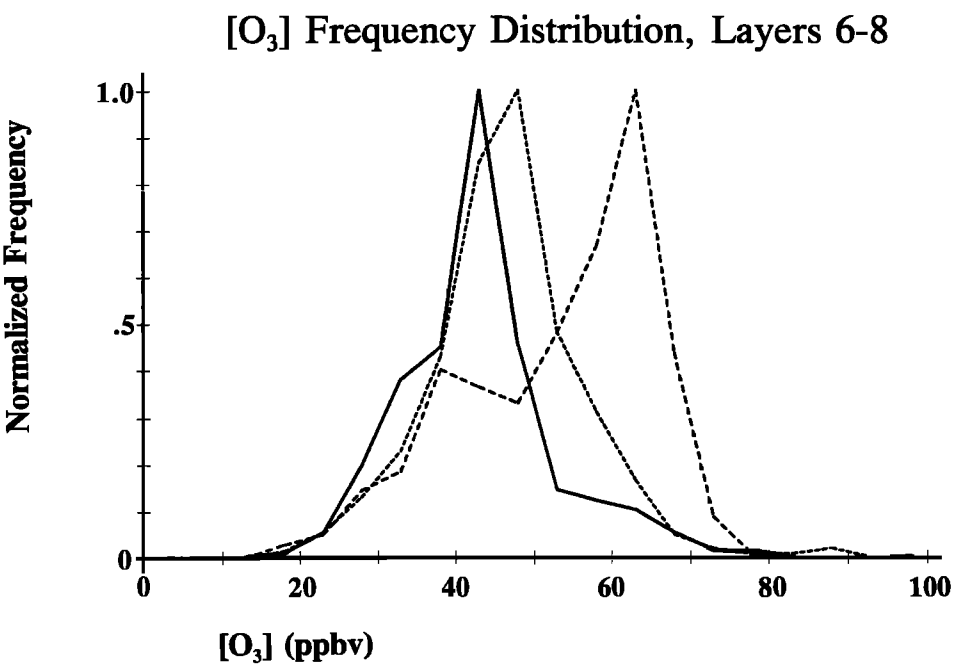

Fig. 13. Same as Figure 11, for the middle troposphere (L6-L8; 4.18-7.98 km).

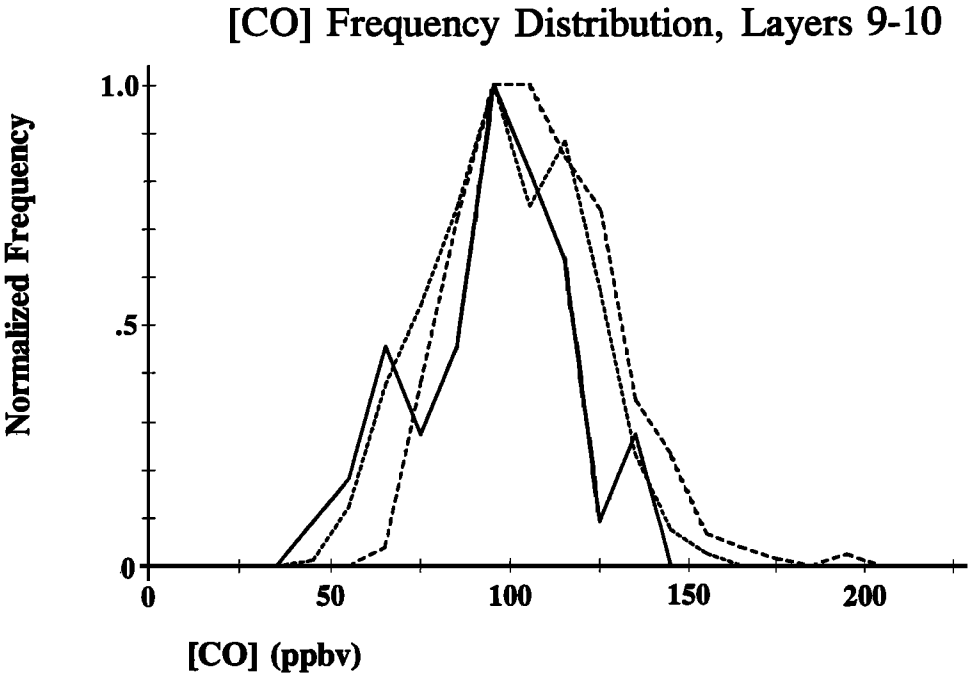

Fig. 14. Same as Figure 10, for the upper troposphere (L9-L10; 7.98-12.0 km).

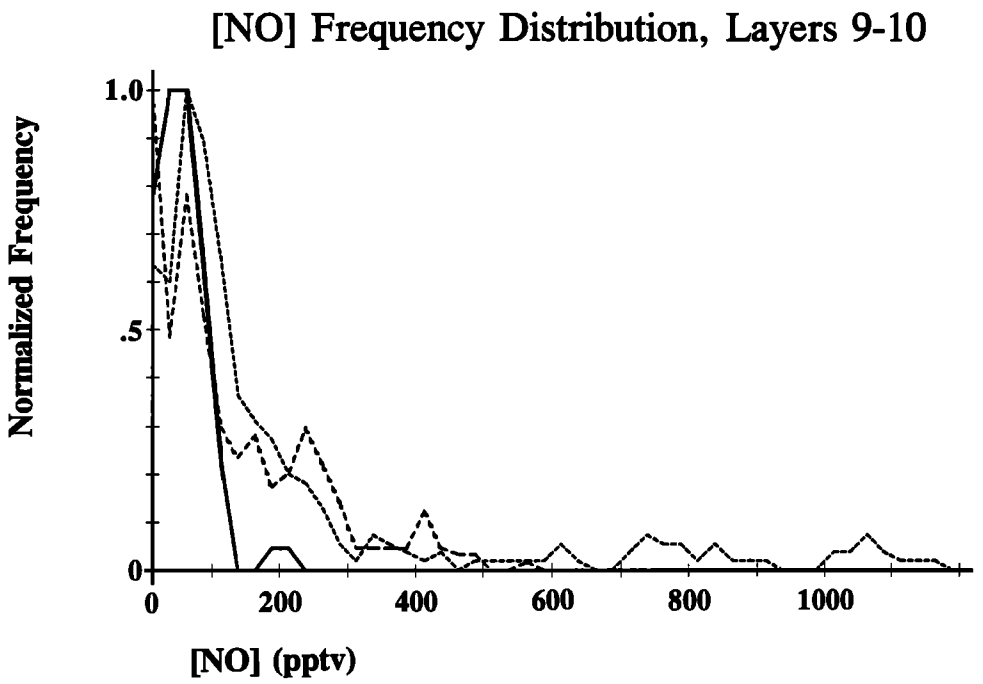

Fig. 15. Normalized frequency distributions of [NO] in the upper troposphere. Solid curve depicts observations in P/P(mod) flow; short-dashed line, mT/mT(mod); and long-dashed line, fropa. The width of each concentration bin is 25 ppt.

maritime [NO_y] histogram peaks at ~750 pptv, typical concentrations in the clear air between growing convective cells or in the preconvective environment. Larger NO_y concentrations (1200-2200 ppt) were observed primarily in the MCS remnants of flights R12 and R13 and in the outflow regions of active cells. By contrast, the narrow fropa [NO_y] distribution peaks at ~700 ppt and displays concentrations of only 500-1400 ppt. The homogeneity of the fropa distribution suggests an atmosphere that is better mixed than in mT or mT(mod) flow; the absence of large NO_y concentrations reflects reduced electrical activity in fropa flow (Table 1).

The highly structured frequency distribution of [O_3] in the upper troposphere under polar flow (Figure 17) reflects the reduced height of the tropopause in the postfrontal environment and the presence of air mixed downward from the lower stratosphere (maximum concentration is 140 ppb). In background air, ozone concentrations frequently ranged from 40 to 45 ppb. The maritime [O_3] distribution also peaks at 40-45 ppb. The principal mode is broader in maritime flow than under polar conditions, however, reflecting both the convective transport of ozone-rich boundary layer air and the limited photochemical production from recently transported precursors. The sharply

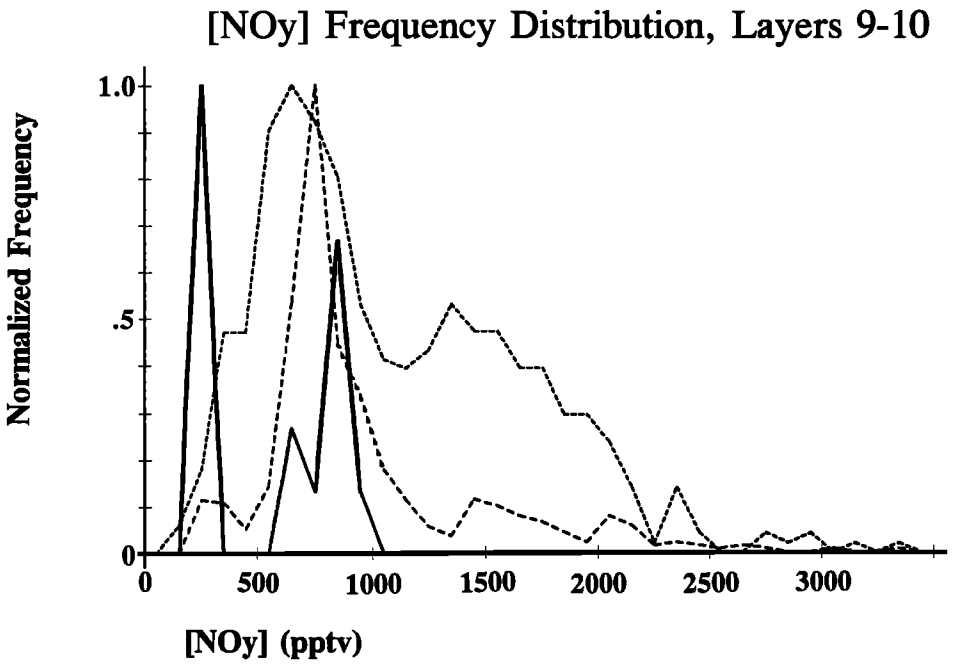

Fig. 16. Normalized frequency distributions of [NOy] in the upper troposphere. Solid curve depicts observations in P/P(mod) flow; short-dashed line, mT/mT(mod); and long-dashed line, fropa. The width of each concentration bin is 100 ppt.

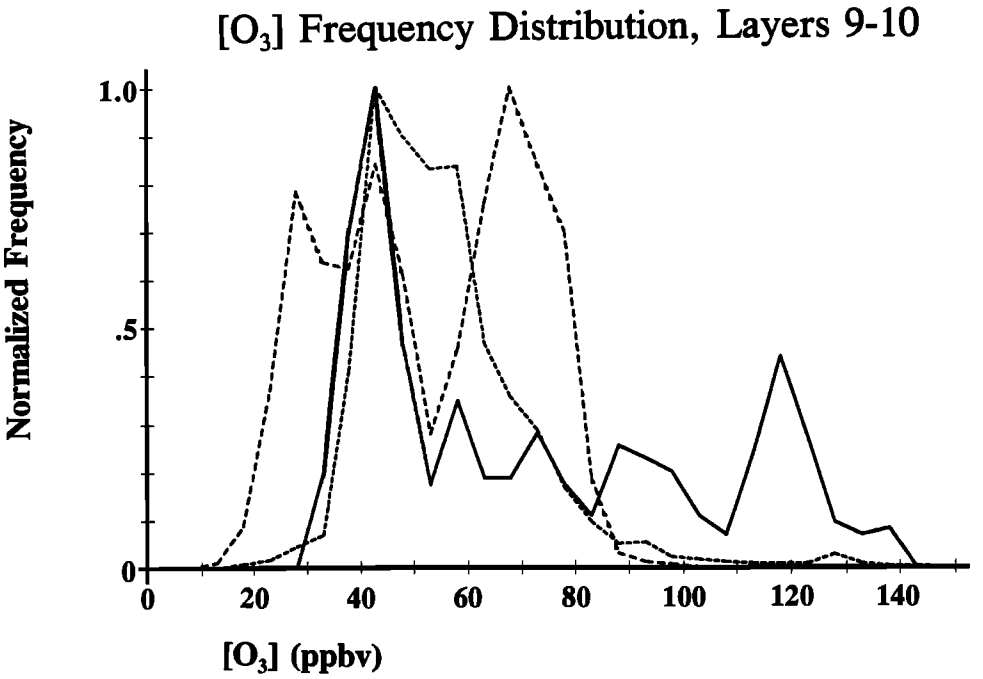

Fig. 17. Same as Figure 11, for the upper troposphere (L9-L10; 7.98-12.0 km).

bimodal fropa [O_3] distribution reflects the degree to which upper tropospheric air is disturbed by convection along the front. Ozone concentrations of 25-45 ppb were measured in air only recently injected into the upper troposphere, while concentrations of 65-70 ppb were produced photochemically from precursors transported earlier.

3.3 *Origins of Free Tropospheric NO*

Instances of high concentrations of NO and other nitrogen species are common in the maritime and frontal passage categories, as depicted in the histograms and altitude profiles discussed above. Lightning, convective transport of polluted PBL air, or downward transport from the stratosphere might cause these elevated readings, and in this section we pursue several lines of reasoning to show which process dominates under each meteorological pattern.

The most dramatic incidents of high concentrations of reactive nitrogen species in the free troposphere were observed as spikes of NO. Lasting 20 to 60 s, these features correspond to plumes 5 to 12 km wide at the typical air speed of the Sabreliner. High levels of NO were also observed as broad features lasting the full 3-min sample period. Figure 18 illustrates typical examples recorded in or around cirrus clouds

in the upper troposphere. The spike (Figure 18*a*) was observed under mT conditions, while the broad feature (Figure 18*b*) was observed under fropa conditions. Narrow features were encountered much more frequently in maritime air (7 of 12 cases) than in air near a cold front (1 of 10 cases) and generally showed no relation with CO or O_3. Broad features, typically observed in fropa flow, were usually accompanied by high [CO]. High [NO] was generally found inside clouds under maritime conditions but between or above clouds in fropa flow. The ratio of maximum concentration of NO relative to the mean concentration of NO_z* measured immediately thereafter was much higher for maritime conditions than for fropa. Finally, the average coefficient of variability of NO data under maritime conditions, 76%, was much higher than under fropa conditions, 28%.

We offer the following hypothesis to explain the differences between these two types of high NO events. Both lightning and upward transport of polluted PBL air contribute to high NO levels in the free troposphere, but in the maritime flow category, lightning dominates, and under fropa flow, upward transport dominates. In neither case is downward transport from the stratosphere important; if it were, then O_3 levels would be greater than are observed. Lightning produces NO but not NO_2 [*Borucki and Chameides*, 1984], so maritime category in-cloud measurements tend to exhibit high levels of recently produced NO which often exceed concentrations of NO_z* in surrounding air and exhibit little correlation with CO. Other investigators have attributed spikes in NO observed in clouds over the ocean to electrical activity [e.g., *Ridley et al.*, 1987; *Davis et al.*, 1987]. On the other hand, transported PBL air typically en-

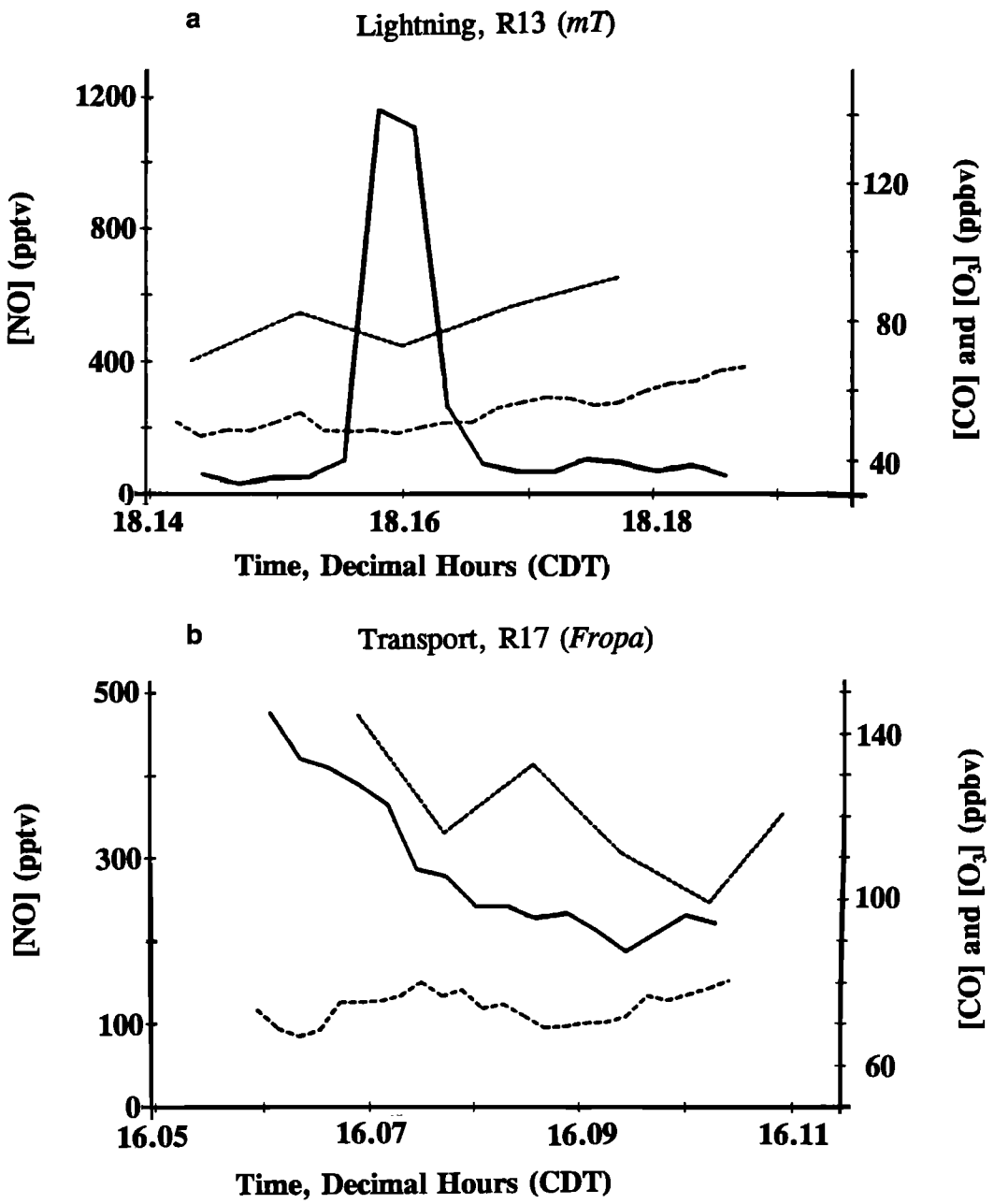

Fig. 18. (*a*) Time series plot of NO, CO, and O_3 mixing ratios encountered at 10.6 km on flight R13 (mT flow) with spike due to lightning. (*b*) Time series plot of NO, CO, and O_3 at 10.0 km during R17 (fropa) where increased trace gas concentrations were more likely produced by upward transport.

countered under fropa conditions contains NO and NO_2 in photochemical steady state. High-altitude NO resulting from transport shows the CO and NO_x* signature characteristic of the PBL, and [NO] is highest where NO_2 photolysis is greatest, above clouds [e.g., *Dickerson et al.*, 1982; *Thompson*, 1984; *Madronich*, 1987; *Walcek et al.*, 1990].

The level of cloud electrical activity is controlled primarily by thunderstorm height [e.g., *Cherna and Stansbury*, 1986; *Orville*, 1990]. In a study of New Mexico thunderstorms, for example, *Dye et al.* [1989] concluded that the onset of electrification and lightning proceeded only after cloud tops reached altitudes of approximately 8 and 9.5 km, respectively. Our aircraft observations and the PRESTORM radar and satellite observations [*Meitín*, 1987] indicate that cloud tops are much higher in the maritime classifications than under fropa conditions. A greater lightning frequency under maritime conditions would thus be expected.

In order to determine whether lightning activity in maritime flow was responsible for the observed enhancement of reactive nitrogen in the free troposphere we examined data collected from a lightning detection network managed by the National Severe Storms Laboratory (NSSL) in Norman, Oklahoma. This network recorded the time and location of lightning flashes over an area that included most of Oklahoma, Kansas, northern Texas, and southern Nebraska [*McGorman and Nielsen*, 1991]. Correlating the observed concentrations of reactive nitrogen species with measured lightning frequencies entails several difficulties, however. Cloud-to-ground flashes were recorded, but the more plentiful cloud-to-cloud flashes were not. Data were not recorded for every flight, and the aircraft sometimes flew outside the area of reliable coverage.

Lightning frequencies recorded over the flight region are listed in Table 1 for the time of the mission and the previous 6 hours (D. McGorman, personal communication, 1991). Bearing in mind the limitations stated above, frequencies are highest under maritime flow conditions, followed by fropa, with polar flow showing little or no lightning. Several flights crossed boundaries, and where both fropa and polar air were encountered, such as on June 27, lightning was seen predominantly in the area of the front. On flights involving both maritime and fropa conditions, lightning was most frequent in a line of convective clouds in maritime air, well ahead of the front. Even if we exclude R15 and R16, in which both mT and fropa conditions were encountered, the lightning detector data strongly support the hypothesis that maritime conditions produce much more lightning than fropa. The average number of flashes was about 70 for fropa conditions and over 1000 for mT/mT(mod).

4. SUMMARY AND CONCLUSIONS

A substantial data set of observed NO, NO_x*, NO_y, CO, and O_3 concentrations from flights over the south central United States in June 1985 has been described. The results were categorized into appropriate phases and subbranches of the meridional circulation over the flight region, as outlined in part 1, and were placed into one of ten equal-mass layers between 0 and 12 km. These observations illustrate the effects of vertical and horizontal atmospheric motions upon trace gas concentrations and tropospheric photochemistry. While several thousand individual trace gas measurements were recorded, only a few flights were made in each flow category and more research is called for.

Impulses of polar air bathe the flight region in clean air from the north and northwest. General subsidence gives rise to a shallow PBL, effectively confining pollutants near the surface. Vertical transport is slow, giving rise to sharp vertical concentration gradients of CO and odd nitrogen species. Vertical profiles of reactive nitrogen compounds describe a "C" shape reflecting stratospheric and surface sources and the dearth of sources in the middle troposphere. The reduced height of the tropopause in the postfrontal environment allowed the Sabreliner to sample air of stratospheric origin, with its characteristic signature of high ozone and odd nitrogen concentrations. In other flow regimes the tropopause lay above the maximum flight level of the Sabreliner. In polar flow a large degree of structure in the frequency distributions of carbon monoxide and odd nitrogen reflects pollution superimposed on cleaner background air. Ozone concentrations are narrowly distributed, however, implying generally slow photochemical production.

In the maritime tropical (mT) category, impulses of southerly flow from the Gulf of Mexico distribute elevated concentrations of carbon monoxide, ozone, and reactive nitrogen compounds throughout a deep mixed layer that extended as high as 4.2 km. The formation and breakup of a deep PBL on successive days may be an important mechanism for lofting photochemically active trace gases into the middle troposphere. CO and O_3 concentrations above the PBL are low, similar to those encountered in polar flow, until layers 9 and 10 where the effects of cloud venting and lightning from widely scattered thunderstorms increase trace gas concentrations.

The capping inversion associated with mT(mod) flow may suppress widespread convective activity but often induces deep, locally focused convection as individual air parcels break through the cap and quickly accelerate upward in the unstable environment. Both the lack of low- and mid-level detrainment in these storms and the reduced burdens of anthropogenic trace species in the southwesterly capping flow result in a clean lower and middle troposphere; carbon monoxide and odd nitrogen concentrations under mT(mod) conditions resemble those measured in polar flow, and ozone levels are lowest of any flow category.

In the upper troposphere in the mT(mod) category, concentrations away from clouds are similar to those observed under polar flow, but near clouds, dramatic enhancement of CO and NO_y is seen. Detrainment from convective storms injects PBL air into the upper troposphere, and lightning adds narrow bands of NO; we recorded one observation of NO above 4 ppb in a thunderstorm. Convective transport may be distinguished from lightning as a source of odd nitrogen in the upper troposphere in several ways. High [NO] from transport is observed over large areas, and is generally accompanied by high [CO]. Reactive nitrogen produced by lightning occurs in narrow plumes, shows little correlation with CO, and frequently exceeds concentrations of NO_x* in surrounding air. In neither case are high mixing ratios of O_3 observed, however. Ozone levels under mT(mod) conditions are similar to those encountered in P(mod) flow, suggesting limited photochemical ozone production from the recently transported precursors. The full effects of photochemistry would presumably be seen well downwind of the flight region.

The layered convection accompanying frontal passage often produces stratiform clouds in which deeper convective cells may be embedded. This layered lifting along a broad front efficiently mixes the troposphere at many levels. In contrast to maritime flow, episodes of frontal passage overturn the troposphere so efficiently that much of the local convection in the flight region injects boundary layer pollutants into air already disturbed by

convection upstream of the flight region. The cumulative effects of such repeated convection produce uniform vertical gradients of long-lived trace species such as CO. Shorter-lived species such as odd nitrogen have minima in the middle troposphere and are enhanced in the outflow of the convection. Cloud electrification is less intense during frontal passage, so that vertical transport plays a greater role than lightning in enhancing odd nitrogen in the FT. Ozone concentrations tend to define bimodal populations at all layers. Lower O_3 concentrations are measured in air only recently injected aloft, while larger concentrations are encountered in air disturbed by repeated convective activity. The efficient transport of lower tropospheric air alters significantly the chemical identity of the middle and upper troposphere and sets the stage for efficient long-range transport of ozone precursors and significant *in situ* photochemical ozone production.

The variation of vertical trace gas distributions with synoptic flow patterns and the resulting horizontal and vertical air mass trajectories illustrate the importance of understanding the effects of convective transport on the chemistry of the troposphere. The difference between trace gas mixing ratios measured in convectively stable flow regimes (P and P(mod)) and those observed in convectively unstable flow can amount to as much as 35-40% for $[O_3]$, 50 % for [CO], and an order of magnitude for odd nitrogen in the middle and upper troposphere. Numerical models of the troposphere using eddy diffusion theory exclusively can seriously underestimate middle and upper tropospheric concentrations of a variety of short-lived trace gases. Global and regional models must realistically parameterize convective transport in order to accurately calculate changes in the atmosphere.

Acknowledgments. The authors would like to thank DOE, NOAA, and NSF who sponsored PRECP/PRESTORM and the many participants of the project who aided in collecting and processing the data, including J. Cunning (NOAA), J. Meitín and D. McGorman (NSSL), and the crew of the NCAR Sabreliner (A. Schanot, J. Pelk, S. Skinner, W. Dawson, R. Burris, J. Ragni, and R. Carl). In addition, we would like to thank A. Delany, B. S. Gockel, A. Fried, W. Dorko, and T. Kelly for their assistance. Special thanks go to Barbara Knowles and Corinne Preston for their assistance in preparing this manuscript. This research was supported primarily by NSF grants ATM-83-05843 and ATM-86-1949-1.88

REFERENCES

Anthes, R. A., Y.-H. Kuo, S. G. Benjamin, and Y.-F. Li, The evolution of the meso-scale environment of severe local storms: Preliminary modelling results, *Mon. Weather Rev., 110*, 1187-1213, 1982.

Bartels, D. L., J. M. Skradski, and R. D. Menard, Mesoscale convective systems: A satellite-data-based climatology, *Tech. Memo. ERL ESG-8*, Nat. Oceanic and Atmos. Admin., Boulder, Colo., 1984.

Boatman, J. F., D. L. Wellman, C. C. Van Valin, R. L. Gunter, J. D. Ray, H. Sievering, Y.Kim, S. W. Wilkison, and M. Luria, Airborne sampling of selected trace chemicals above the central United States, *J. Geophys. Res., 94*, 5081-5094, 1989.

Boatman, J. F., N. Laulainen, J. Ray, C. Van Valin, L. Gunter, R. Lee, D. Luecken, and K. Busness, Acid precursor concentrations above the northeastern United States during summer 1987: Three case studies, *J. Geo-phys. Res., 95*, 11,831-11,846, 1990.

Borucki, W. J., and W. L. Chameides, Lightning: Estimates of the rates of energy dissipation and nitrogen fixation, *Rev. Geophys. Space Phys., 22*, 363-372, 1984.

Carlson, T. N., and F. H. Ludlam, Conditions for the occurrence of severe local storms, *Tellus, 20*, 203-226, 1968.

Carlson, T. N., S. G. Benjamin, G. S. Forbes, and Y.-F. Li, Elevated mixed layers in the regional severe storm environment: Conceptual model and case studies, *Mon. Weather. Rev., 111*, 1453-1473, 1983.

Carroll, M. A., M. McFarland, B. A. Ridley, and D. L. Albritton, Ground-based nitric oxide measurements at Wallops Island, Virginia, *J. Geophys. Res., 90*, 12,853- 12,860, 1985.

Carroll, M. A., et al., Aircraft measurements of NO_x over the Eastern Pacific and continental United States and implications for ozone production, *J. Geophys. Res., 95*, 10,205- 10,234, 1990.

Chameides, W. L., and R. J. Cicerone, Effects of nonmethane hydrocarbons in the atmosphere, *J. Geophys. Res., 83*, 947-952, 1978.

Chameides, W. L., D. H. Stedman, R. R. Dickerson, D. W. Rusch, and R. J. Cicerone, NO_x production in lightning, *J. Atmos. Sci., 34*, 143-149, 1977.

Chameides, W. L., D. D. Davis, M. O. Rodgers, J. Bradshaw, S. Sandholm, G. Sachse, G. Hill, G. Gregory, and R. Rasmussen, Net ozone photochemical production over the eastern and central North Pacific as inferred from GTE/CITE 1 observations during fall 1983, *J. Geophys. Res., 92*, 2131-2152, 1987*a*.

Chameides, W. L., D. D. Davis, J. Bradshaw, M. O. Rodgers, S. Sandholm, and D. B. Bai, An estimate of the NO_x production in an electrified cloud based on NO observations from the GTE/CITE 1 fall 1983 field observations, *J. Geophys. Res., 92*(2), 2153-2156, 1987*b*.

Cherna, E. V., and E. J. Stansbury, Sferics rate in relation to thunderstorm dimensions, *J. Geophys. Res., 91*, (B) 701-707, 1986.

Condon, E. P., E. F. Danielson, G. W. Sachse, and G. W. Hill, Carbon monoxide measure-ments over the eastern Pacific during GTE/CITE 1, *J. Geophys. Res., 92*, 2095-2104, 1987.

Crutzen, P. J., and L. T. Gidel, A two-dimensional photochemical model of the atmosphere, 2, The tropospheric budgets of the anthropogenic chlorocarbons CO, CH_4, CH_3Cl and the effect of various NO_x sources on tropospheric ozone, *J. Geophys. Res., 88*, 6641- 6661, 1983.

Danielsen, E. F., Stratospheric-tropospheric exchange based on radioactivity, ozone and potential vorticity, *J. Atmos. Sci., 25*, 502- 518, 1968.

Daum, P. H., L. I. Kleinman, A. J. Hills, A. L. Lazrus, A. C. D. Leslie, K. Busness, and J. Boatman, Measurement and interpretation of concentrations of H_2O_2 and related species in the upper Midwest during summer, *J. Geophys. Res., 95*, 9857-9871, 1990.

Davis, D. D., J. D. Bradshaw, M. O. Rodgers, S. T. Sandholm, and S. Kesheng, Free tropospheric and boundary layer measurements of NO over the central and eastern North Pacific Ocean, *J. Geophys. Res., 92*, 2049-2070, 1987.

Delany, A. C., R. R. Dickerson, F. L. Melchior, Jr., and A. F. Wartburg, Modification of a commercial NO_x detector for high sensitivity, *Rev. Sci. Instrum., 53*, 1899-1902, 1982.

Dickerson, R. R., Measurements of reactive nitrogen compounds in the free troposphere, *Atmos. Environ., 18*, 2585-2593, 1984.

Dickerson, R. R., Reactive nitrogen compounds in the Arctic, *J. Geophys. Res., 90*(6), 10,739-10,743, 1985.

Dickerson, R. R., and A. C. Delany, Modification of a commercial gas filter correlation CO detector for enhanced sensitivity, *J. Atmos. Oceanic Technol., 5*, 424-431, 1988.

Dickerson, R. R., D. H. Stedman, and A. C. Delany, Direct measurements of ozone and nitrogen dioxide photolysis rates in the troposphere, *J. Geophys. Res., 87*(7), 49334946, 1982.

Dickerson, R. R., A. C. Delany, and A. F.Wartburg, Further modification of a commercial NO_x detector for high sensitivity, *Rev. Sci. Instr., 55*(12), 1995-1998, 1984.

Dickerson, R. R., et al., Thunderstorms: An important mechanism in the transport of air pollutants, *Science, 235*, 460-465, 1987.

Drummond, J. W., A. Volz, and D. H. Ehhalt, An optimized chemiluminescent detector for tropospheric NO measurements, *J. Atmos. Chem., 2*, 287-306, 1985.

Drummond, J. W., D. H. Ehhalt, and A. Volz, Measurements of nitric oxide between 0-12 km altitude and 67°N to 60°S latitude obtained during STRATOZ III, *J. Geophys. Res., 93*, 15,831-15,849, 1988.

Dye, J. E., W. P. Winn, J. J. Jones, and D. W. Breed, The electrification of New Mex-ico thunderstorms, 1, Relationship between precipitation development and the onset of electrification, *J. Geophys. Res., 94*, 8643- 8656, 1989.

Fehsenfeld, F. C., et al., A ground-based intercomparison of NO, NO_z, and NO_y measurement techniques, *J. Geophys. Res., 92*, 14,710-14,722, 1987.

Fehsenfeld, F. C., D. D. Parrish, and D. W.Fahey, The measurement of NO_z in the non-urban troposphere, in *NATO Workshop on Tropospheric Ozone: Regional and Global Ozone and Its Environmental Consequences*, edited by I. Isaksen, D. Reidel, Norwell, Mass., 1988.

Fontijn, A., A. J. Sabadell, and R. J. Ronco, Homogeneous chemiluminescent measurement of nitric oxide with ozone: Implications for continuous selective monitoring of gaseous air pollutants, *Anal. Chem., 42*, 575-579, 1970.

Greenberg, J. P., P. R. Zimmerman, and P. Haagenson, Tropospheric hydrocarbon and CO profiles over the U. S. West Coast and Alaska, *J. Geophys. Res., 95*, 14,015- 14,026, 1990.

Hastie, D. R., H. Schiff, D. M. Whelpdale, R. E. Peterson, and W. H. Zoller, Nitrogen and sulphur over the western Atlantic Ocean, *Atmos. Environ., 22*(11), 2381-2391, 1988.

Heidt, L. E., J. P. Krasnec, R. A. Lueb, W.H. Pollock, B. E. Henry, and P. J. Crutzen, Latitudinal distributions of CO and CH_4 over the Pacific, *J. Geophys. Res., 85*, 7329-7336, 1980.

Heikes, B. G., G. L. Kok, J. G. Walega, and A. L. Lazrus, H_2O_2, O_3, and SO_2 measurements in the low troposphere over the eastern United States during Fall, *J. Geophys. Res., 92*, 915-931, 1987.

Hübler, G., D.W. Fahey, B.A. Ridley, G.L. Gregory, and F.C. Fehsenfeld, Airborne measurements of total reactive odd nitrogen (NO_y), *J. Geophys. Res., 97*, 9833-9850, 1992.

Hughes, E. E., A. J. Davenport, P. T. Woods, W. L. Zielinski, Intercomparison of a range of primary gas standards of CO in N_2 and CO_2 in N_2 prepared by the National Institute of Standards and Technology and the National Physical Laboratory, *Environ. Sci. Technol., 24*(4), 671-676, 1991.

Junge, C. E., Residence time and variability of tropospheric trace gases, *Tellus, 26*, 477- 488, 1974.

Kelly, T. J., D. H. Stedman, J. A. Ritter, and R. B. Harvey, Measurements of oxides of nitrogen and nitric acid in clean air, *J. Geophys. Res., 85*, 7417-7425, 1980.

Kley, D., J. W. Drummond, M. McFarland, and S. C. Liu, Tropospheric profiles of NO_y, *J. Geophys. Res., 86*, 3153-3161, 1981.

Kondo, Y., W. A. Matthews, A. Iwata, Y. Morita, and M. Takagi, Aircraft measurements of oxides of nitrogen along the eastern rim of the Asian continent: Winter observations, *J. Atmos. Chem., 5*, 37-58, 1987.

Liu, S. C., M. Trainer, F. C. Fehsenfeld, D. D. Parrish, E. J. Williams, D. W. Fahey, G. Hübler, and P. C. Murphy, Ozone production in the rural troposphere and the implications for regional and global ozone distributions, *J. Geophys. Res., 92*(D4), 4191-4207, 1987.

Logan, J. A., M. J. Prather, S. C. Wofsy, and M. B. McElroy, Tropospheric chemistry: A global perspective, *J. Geophys. Res., 86* (C8), 7210-7254, 1981.

Luke, W. T., Reactive Nitrogen Compounds in the Troposphere: Observations, Transport, and Photochemistry, Ph.D. dissertation, Dep. of Chem., Univ. of Md., College Park, 1990.

Luke, W. T., and R. R. Dickerson, The flux of reactive nitrogen compounds from eastern North America to the western Atlantic Ocean, *Global Biogeochem. Cycles., 1*, 1329-344, 1987.

Madronich, S., Photodissociation in the atmosphere, 1, Actinic flux and the effects of ground reflections and clouds, *J. Geophys. Res., 92*, 9740-9752, 1987.

Marenco, A., M. Macaigne, and S. Prieur, Meridional and vertical CO and CH_4 distributions in the background troposphere (70N-60S; 0-12 km altitude) from scientific aircraft measurements during the STRATOZ III experiment (June 1984), *Atmos. Environ., 23*, 185-200, 1989.

McGorman, D. R., and K. E. Nielsen, Cloud-to-ground lightning in a tornadic storm on 8 May 1986, *Mon. Weather Rev. 119,*, 1557-1574, 1991.

McNamara, D. P., Origin of Ozone over Central U.S., M.S. thesis, Dep. of Meteorol., University of Md., College Park, 1988.

Meitin, J. G., Jr., The Oklahoma-Kansas Preliminary Regional Experiment for STORM-CENTRAL (O-K PRE-STORM), vol. 2 Radar Data Summary, *Tech. Memo., ERL ESG-26*, 84 pp., Nat. Oceanic and Atmos. Admin., 1987.

Misanchuk, B. A., D. R. Hastie, and H. I. Schiff, The distribution of nitrogen oxides off the East Coast of North America, *Global Biogeochem. Cycles., 1*, 345-356, 1987.

Moncrieff, M. W., Dynamical models of the transport of momentum, mass, and inert tracers by mesoscale convective systems, in *Proceedings of the Symposium on the Role of Clouds in Atmospheric Chemistry and Global Climate*, pp. 264-269, Amererican Meteorological Society, Boston, Mass., 1989.

NOAA, U. S. Standard Atmosphere, 1976, Rep. NOAA-S/T76-1562, 1976.

Nunnermacker, L. J., Calibration and detection of reactive nitrogen compounds in the atmosphere, Ph.D. dissertation, Dep. of Chem., Univ. of Md., College Park, 1990.

Orville, R. E., Peak-current variations of lightning return strokes as a function of latitude, *Nature, 343*, 149-151, 1990.

Pickering, K. E., Observations of tropospheric trace gases and innovative techniques for assessing regional transport of air pollutants, Ph.D. dissertation, Dep. of Meteorol., Univ. of Md., College Park, 1987.

Pickering, K. E., R. R. Dickerson, G. J.Huffman, J. F. Boatman, and A. Schanot, Trace gas transport in the vicinity of frontal convective clouds, *J. Geophys. Res., 93*, 759-773, 1988.

Pickering, K. E., R. R. Dickerson, G. J. Huffman, W. T. Luke, and L. J. Nunner-macker, Clear-sky vertical profiles of trace gases as influenced by upstream convective activity, *J. Geophys. Res., 94*, 14,875-14,892, 1989.

Pickering, K. E., A. M. Thompson, R. R. Dickerson, W. T. Luke, D. P. McNamara, J. P. Greenberg, and P. R. Zimmerman, Model calculations of tropospheric ozone production potential following observed convective events, *J. Geophys. Res., 95*, 14,049-14,062, 1990.

Pickering, K. E., A. M. Thompson, J. R. Scala, W-K. Tao, J. Simpson, and M. Garstang, Photochemical ozone production in tropical squall line convection during NASA Global Tropospheric Experiment/Amazon Boundary Layer Experiment 2A, *J. Geophys. Res., 96*(2), 3099-3114, 1991.

Ridley, B. A., M. A. Carroll, and G. L. Gregory, Measurements of nitric oxide in the boundary layer and free troposphere over the Pacific Ocean, *J. Geophys. Res., 92*, 2025-2047, 1987.

Ridley, B. A., et al., Ratios of peroxyacetyl nitrate to active nitrogen observed during aircraft flight over the eastern Pacific Ocean and continental United States, *J. Geophys. Res., 95*, 10,179-10,192, 1990.

Ryan, W. F., Synoptic scale variations in vertical ozone profiles over the lower Great Plains of the United States, M.S. thesis, Dep. Meteorol., Univ. of Md., College Park, 1990.

Ryan, W. F., R. R. Dickerson, G. J. Huffman, and W. T. Luke, Tropospheric chemistry over the lower Great Plains of the United States, 1, Meteorology, *J. Geophys. Res., 97(D16)*, 17,963-17,984, 1992.

Seiler, W., and J. Fishman, The distribution of carbon monoxide and ozone in the free troposphere, *J. Geophys. Res., 86*, 7255-7265, 1981.

Singh, H. B., and P. L. Hanst, Peroxyacetyl nitrate (PAN) in the unpolluted atmosphere: An important reservoir for nitrogen oxides, *Geophys. Res. Lett., 8*, 941-944, 1981.

Singh, H. B., and L. J. Salas, Methodology for the analysis of peroxyacetyl nitrate (PAN) in the unpolluted atmosphere, *Atmos. Environ., 17*, 1507-1516, 1983.

Singh, H. B., et al., Relationship between peroxyacetyl nitrate (PAN) and nitrogen oxides in the clean troposphere, *Nature, 318*, 347-348, 1985.

Stedman, D. H., A flow independent procedure for the gas phase titration of an ozone source, *J. Air Pollut. Control Assoc., 26*, 62, 1976.

Stedman, D. H., and M. J. McEwan, Oxides of nitrogen at two sites in New Zealand, *Geophys. Res. Lett., 10*, 168-171, 1983.

Stedman, D. H., E. E. Daby, F. Stuhl, and H. Niki, Analysis of ozone and nitric oxide by a chemiluminescent method in laboratory and atmospheric studies of photochemical smog, *J. Air Pollut. Control Assoc., 22*, 260-263, 1972.

Thompson, A. M., The effect of clouds on photolysis rates and ozone formation in the unpolluted tropsphere, *J. Geophys. Res., 89*, 1341-1349, 1984.

Thompson, A. M., and R. J. Cicerone, Possible perturbations to atmospheric CO, CH_4, and OH, *J. Geophys. Res., 91*, 10,853-10,864, 1986.

Torres, A. L., and H. Buchan, Tropospheric-nitric oxide measurements over the Amazon basin, *J. Geophys. Res., 93*, 1396-1406, 1988.

Trainer, M., E. J. Williams, D. D. Parrish, M. P. Buhr, E. J. Allwine, H. H. Westberg, F. C. Fehsenfeld, and S. C. Liu, Models and observations of the impact of natural hydrocarbons on rural ozone, *Nature, 329*, 705-707, 1987.

Van Valin, C., and M. Luria, O_3, CO, hydrocarbons and dimethyl sulfide over the western Atlantic Ocean, *Atmos. Environ. 22*(11), 2401-2409, 1988.

Van Valin, C., M. Luria, J. D. Ray, and J. F. Boatman, Hydrogen peroxide and ozone over the northeastern United States in June 1987, *J. Geophys. Res., 95*, 5689-5696, 1990.

Walcek, C. J., W. R. Stockwell, and J. S. Chang, Theoretical estimates of the dynamical, radiative, and chemical effects of clouds on tropospheric trace gases, *Atmos. Res., 25*, 53-69, 1990.

R. Dickerson and W. F. Ryan, Department of Meteorology, University of Maryland, College Park, Md 20742.

W. T. Luke, NOAA, Air Resources Laboratory, SSMC II, Rm. 9390, 1325 East-West Highway, Silver Spring, Md 20910.

L. J. Nunnermacker, Environmental Chemistry Division, Dept. of Applied Science, Brookhaven National Laboratory, Upton, NY 11973.

K. E. Pickering, Universities Space Research Association, NASA Goddard Space Flight Center, Greenbelt, Md 20771.

(Received June 26, 1991;
revised July 18, 1992;
accepted August 17, 1992.)